UNIVERSITÄTSKLINIKUM HAMBURG-EPPENDORF

Universitäres Herzzentrum Hamburg
Klinik und Poliklinik für Allgemeine und Interventionelle Kardiologie
Molekulare Kardiologie - Genomik und Systembiologie

Prof. Dr. rer. nat. Tanja Zeller

The role of the NLRC4 inflammasome in the pathogenesis of coronary disease: The influence of genetic variations

Dissertation

zur Erlangung des Grades eines Doktors der Medizin
an der Medizinischen Fakultät der Universität Hamburg.

vorgelegt von:

Simon Zeller
aus Hamburg

Hamburg 2019

Angenommen von der
Medizinischen Fakultät der Universität Hamburg am: 20.02.2020

Veröffentlicht mit Genehmigung der
Medizinischen Fakultät der Universität Hamburg.

Prüfungsausschuss, der/die Vorsitzende: **Prof. Dr. Tanja Zeller**

Prüfungsausschuss, zweite/r Gutachter/in: **Prof. Dr. Kerstin Kutsche**

1 Introduction

1.1 Coronary Artery Disease (CAD)

Coronary artery disease (CAD) is the leading cause of death globally and accounts for 17.3 million deaths per year. Risk factors like obesity have rapidly been increasing, leading to an assumed number of 23.6 million deaths due to CAD by 2030 (Laslett et al., 2012). Current epidemiologic studies determined a 63.3% prospective lifetime risk at the age of 30 for the development of CAD (Rapsomaniki et al., 2014). For the population, aged 50 years and older CAD remains to be the leading cause of death (Lozano et al., 2012). The most common cause for CAD is atherosclerosis, in which thickening of the arteries intimal wall (intima) occurs due to migration of cells, lipids and debris leading to progressive occlusion of the vessels lumen. Risk factors for atherosclerosis include metabolic disorders like diabetes mellitus, obesity, nutrition, physical inactivity, hypertension, dyslipidemia, gender and age (Yahagi et al., 2015). Severe vessel occlusion leads to ischemia and subsequent necrosis of the myocardium (myocardial infarction). Necrotic myocardial tissue changes to fibrotic scar-tissue by inflammation and collagen deposition (fibrosis). Not fully understood, the pathophysiology of CAD development changed from being solitary driven by high levels of Low-density-lipoproteins (LDL) including cholesterol and their deposition in arterial wall layers, to a far more complex combination of an unhealthy lifestyle, genetic predisposition and inflammatory or hormonal processes (Hansson, 2005).

1.2 Inflammation and atherosclerosis

Research continues to focus on how various immunity-derived mechanisms affect stages of disease progression in CAD (Libby et al., 2002, Ikeda, 2003, Hansson, 2005, Hansson and Libby, 2006, De Caterina et al., 2016). Cellular and humoral components of the immune system are involved in the progression of cardiovascular diseases. The primary cell types contributing to disease-development are monocytes and macrophages, but also endothelial and smooth muscle cells are crucial (Ross, 1995, Bjorkbacka, 2015). In addition to cells, the immune system comprises a humoral component providing the necessary plasma proteins for sufficient immune responses. In total, the immune systems can be distinguished in antibodies, the complement-system and interleukins. Recent understanding of the CAD pathophysiology and

especially arterial plaque development show that also microbial pathogens, autoantigens and inflammatory molecules lead to activation and migration of macrophages, and T lymphocytes into the intimal layer. Macrophages are known to incorporate LDL, occurring more likely after LDL-modification through oxidative stress (Linton et al., 2000). Migrated macrophages and smooth muscle cells may transform into foam cells and remain within the arterial wall, resulting in the formation of fibrotic plaques. Additionally cell debris, proteoglycans and hydroxyapatite, proteases, pro-thrombotic factors, secretion of inflammatory cytokines as interleukin (IL)-1ß and IL-18 (Mallat et al., 2001) and Tumour Necrosis Factors (TNFs) moderate plaque formation. When exposed to biomechanical stress, plaque rupture and vessel occlusion may occur, resulting in critical events of ischemia. In summary, the interaction of migrated immune-cells with existing deposits within the vessels wall, as well as inflammatory processes like cytokine release and enzyme activities, lead to the formation of cardiac plaque (Hansson, 2005).

1.2.1 Cell-types important for CAD and relation to this study

Monocytes and macrophages

Diverse cell types like endothelial cells, smooth muscle cells or white blood cells are involved in the development of atherosclerosis. White blood cells, in particular, may migrate into the vascular wall, causing inflammation and signalling lymphocyte-recruitment. Within disease development, fatty streaks (see figure 1.1) represent the first stage of atherosclerosis, but without the necessity of further disease progression. I.e., juvenile vessels may already present fatty streaks, being the result of leucocyte migration into the intimal wall layer (Stary, 1994). Major leucocytes involved are macrophages and monocytes (precursor). Monocytes are circulating leucocytes participating in the specific and non-specific defence system by phagocytosis of foreign bodies, as well as activation of the acquired immune defence by antigen presentation. After differentiation to macrophages, they harvest cellular debris, microbes, foreign substances and others, including oxidative modified LDL (oxLDL). Macrophages are phenotypically distributed into M1 (pro-inflammatory macrophages) or M2 (anti-inflammatory macrophages) promoting Th1 and Th2 responses, respectively. Both cell-types are crucial within CAD development by causing and modulating inflammation when migrated into the vessels wall and further recruit lymphocytes, thus contributing to plaque formation. They may remain within the vessels-wall, perpetuate local inflammation and show altered function when homeostasis in cell-interaction is

disturbed (Linton et al., 2000, Libby et al., 2002, Hansson, 2005, Moore et al., 2013). Under normal conditions, macrophages can take up LDL through LDL receptors (LDL-R), process it into, i.e. cholesterol and re-issue its efflux. In case of atherosclerosis, macrophages also take oxLDL up, leading to excessive over-accumulation of intracellular oxidized lipids. Subsequently, macrophages differentiate into foam cells, enter apoptosis and liberate apoptotic bodies as well as diverse cytokines like Interleukin 18 (IL-18) into plaque-area (Linton et al., 2000, Shashkin et al., 2005). New understanding of disease pathology postulates plasticity of other cells like smooth muscle cells (SMCs), also processing oxLDL and differentiating into foam cells under appropriate circumstances (Bjorkbacka, 2015, Weidmann et al., 2015).

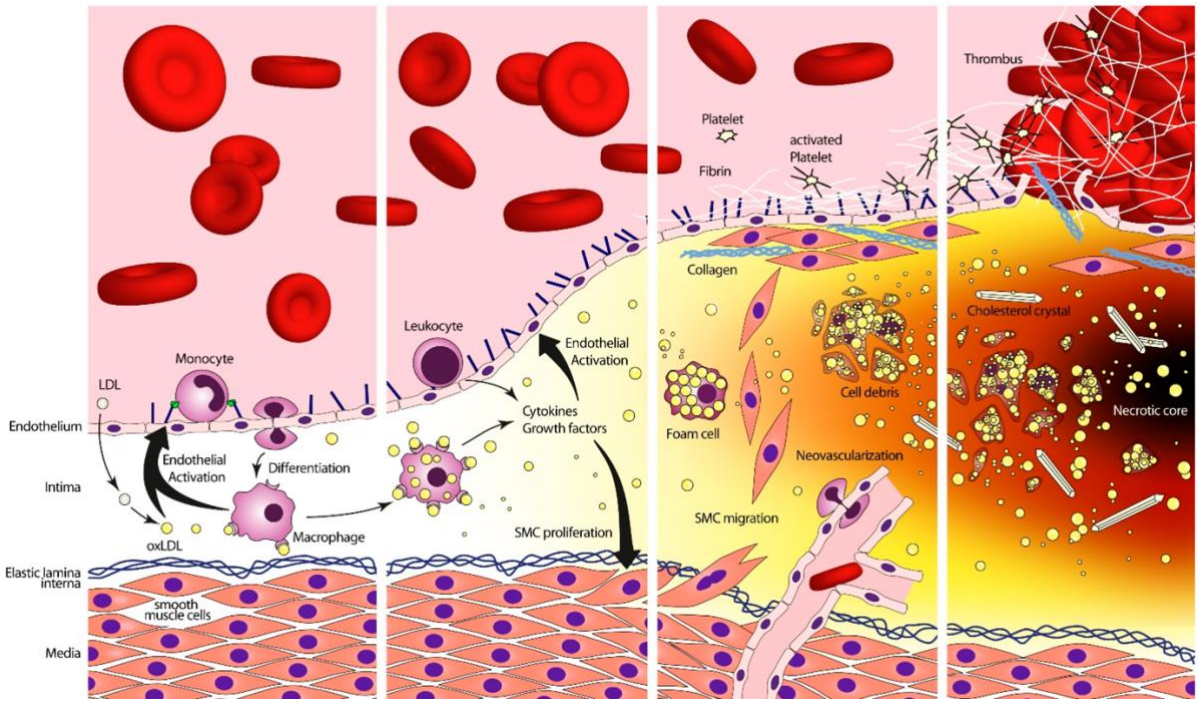

Figure 1.1: Overview of migration of macrophages and differentiation to foam cells in atherosclerotic plaque lesions. From left to right: Lesion initiation; Fatty streak; Fibrous plaque; Thrombosis. Adapted and modified from 'Ultrasound Imaging for Risk Assessment in Atherosclerosis' (Steinl and Kaufmann, 2015)

1.2.2 Cytokines

Cytokines are regulatory polypeptides that mediate signal transduction between cells and influence proliferation and differentiation either in an endocrine (through the bloodstream), a paracrine (direct effect on neighbour-cells) or an autocrine (self-

stimulation) fashion. In vivo cytokine-concentrations are within picomolar (10-12 M) range, but if necessary, i.e. in the context of a trauma or an infection, increase to a 10_3-fold of their baseline-concentration. Cytokines may be summarized either by function or structure, with two or four major categories, respectively. In function, type 1 cytokines are associated to regulation of cellular immune responses (i.e. interferon [IFN]-γ, TNF-α), while on the other hand type 2 cytokines regulate antibody-production (i.e. transforming growth factor β [TGF-β], IL-4, IL-10, IL-13). Regarding the structure, significant subfamilies are IL-1 family, IL-17 family, alpha-helix bundle family (includes IL-2 subfamily, IFN subfamily, and IL-10 subfamily), and cysteine-knot cytokines (TGF-ß superfamily) (Ramani et al., 2015).

1.2.3 Interleukins

Interleukins are a group of cytokines mainly produced and secreted by leucocytes. The effect of interleukins is pleiotropic since they influence other leucocytes to differentiate, divide or on the contrary, inhibit these processes. Inducing secretion occurs due to physiological or non-physiological stimuli (Ramani et al., 2015, Dinarello, 2018). The pro-inflammatory influence of interleukins on CAD development was recently investigated within the Canakinumab Anti-Inflammatory Thrombosis Outcomes Study (CANTOS). In this study, the interleukin-1ß immunity pathway was targeted with the monoclonal antibody Canakinumab and showed a protective effect on the hazard of recurring cardiovascular events in patients with prior myocardial infarction by reduction of inflammation. Pro-inflammatory IL-1β influences the development of atherothrombotic plaque by inducing mono- and leukocyte adhesion the endothelial cells and processes of thrombosis. The findings proofed the inflammatory hypothesis of atherothrombosis and the independent role of inflammation in CAD development (Ridker et al., 2017).

The role of IL-18 (also INF-γ inducing factor (IGIF)) in CAD emerged, when elevated levels of IL-18 in plasma and plaque tissue showed an association to increased cardiac plaque formation and instability (Mallat et al., 2001, Mallat et al., 2002). IL-18 belongs to the Interleukin-1 (IL-1) subfamily and is expressed by Kupffer cells and activated macrophages. It is a pleiotropic mediator capable of inducing the formation of interferon γ as well as GM-CSF and IL-2 in T lymphocytes. IL-18 is activated by caspase-1 through proteolytic maturation and promotes the proliferation of T lymphocytes through an IL-2-dependent mechanism and the activity of NK cells. It is involved in the development of TH1 cells and enhances their cytotoxicity (Dinarello and

Fantuzzi, 2003, Okamura et al., 1995). The IL-18 system consisting of IL-18, IL-18 Receptor 1 (IL-18R1) and IL-18 binding protein (IL-18BP). Genetic studies linked variants on two chromosomal loci to circulating IL-18 concentrations: The *IL18-BCO2* locus on Chr. 11 (Tiret et al., 2005, He et al., 2010) and more recently the *NLCR4* (NOD-, LRR- and CARD-containing 4, otherwise known as IPAF, CARD12) locus on Chr. 2 (He et al., 2010, Matteini et al., 2014, Ahola-Olli et al., 2017), suggesting also a casual linkage between genetic loci and IL-18 maturation. Clinical investigations on IL-18 also proved it to be a predictive biomarker for the outcome of patients with severe myocardial infarction (MI) (Blankenberg et al., 2002, Blankenberg et al., 2003, Chen et al., 2007, Salomaa et al., 2010, Jefferis et al., 2011).

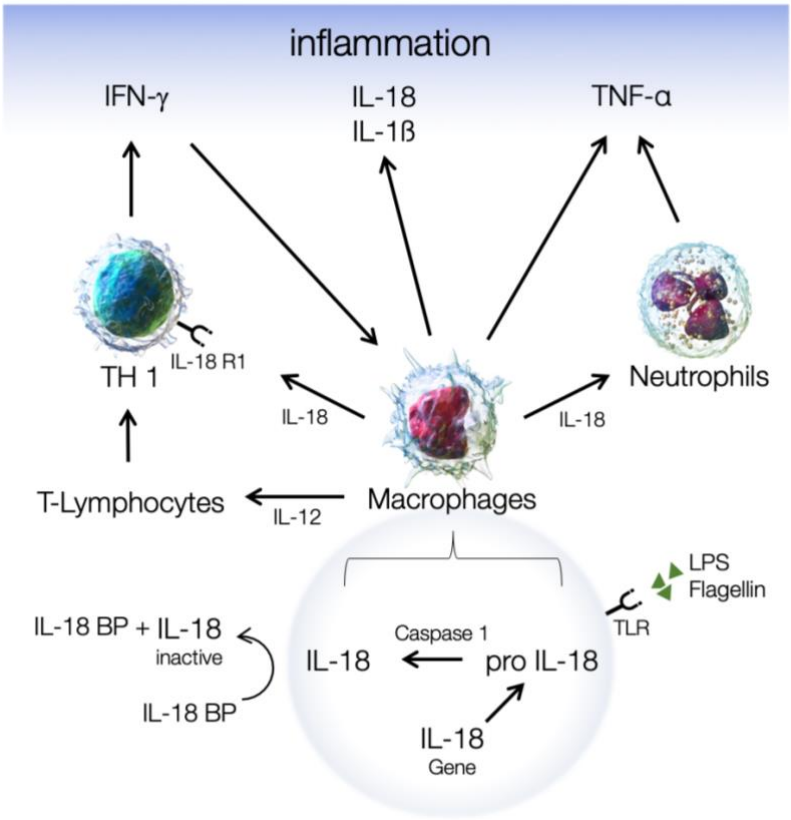

Figure 1.2: Simplified overview of the IL-18 system. Stimuli like LPS lead to IL-18 maturation in, e.g. macrophages. The emitted IL-18 influences different cells like white blood cells in a pro-inflammatory manner and contributes to a global inflammatory response. In part adapted from (Nakanishi et al., 2001), 3D illustration of white blood cells taken from 'Medical Gallery of Blausen Medical' (Bruce Blaus, 2014).

1.2.4 Inflammasomes and NLRC4

Inflammasomes are cytosolic oligo-protein-complexes participating in innate and adapted immune response located in macrophages and neutrophilic granulocytes. By regulation of, i.e. pro-inflammatory enzyme caspase-1, inflammasomes modulate processing and release of cytokines as well as the initiation of pyroptosis, a lytic and inflammatory form of programmed cell death for eukaryotic cells. Assembly and activation of the inflammasome are established when exposed exogenous or endogenous stress (Martinon et al., 2002, Broz, 2015, Monie, 2017). Central components of the inflammasome are among others NOD-like receptors (NLRP1, NLRP3, NLRC4) reacting to pathogen-associated molecular patterns (PAMPs), i.e. due microbial infections, but also damage-associated molecular patterns (DAMPs) as in tissue damage (Bergsbaken et al., 2009, Strowig et al., 2012, Franchi et al., 2009). The NLR-inflammasome subfamily (NLRP1, NLRP3, NLRC4) has a central oligomerization-moderating Nucleotide Binding Domain (NBD, otherwise also NACHT), a c-terminal Leucine-Rich Repeat Domain (LRR) for P- or DAMP recognition, and either Pyrin- (PYD) or caspase activation and recruitment-domains (CARD) in common. CARD and further also PYD are death fold domains, that enable protein-protein interaction with caspase-1 through dimerization with caspase-1's CARD domain.

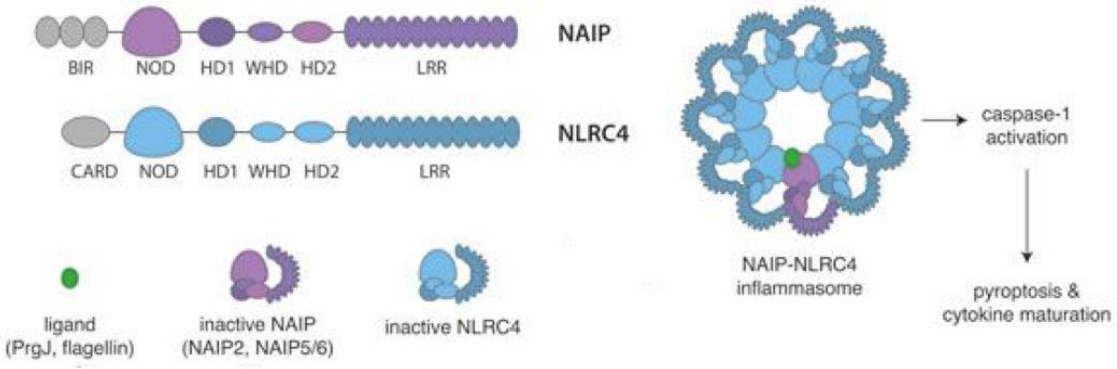

Figure 1.3: Domain organization of NAIPs and NLRC4. NAIP-ligand complex subsequently interacts with inactive NLCC4 molecule, inducing a conformational change that activates NLRC4. Active NLRC4 molecules recruit and activate other NLRC4 molecules in a domino-like reaction. Total NAIP-NLRC4 inflammasome is a multi-subunit disk-like structure containing 9-11 molecules of NLRC4, but only one NAIP molecule. BIR = Baculovirus Inhibitor of apoptosis protein Repeat; NOD = nucleotide-binding and oligomerization domain; HD1 = helical domain 1; WHD = winged-helical domain; HD2 = helical domain 2; LRR = leucine-rich

repeats; CARD = caspase-recruitment domain. Adapted and modified from ‘Inflammasome assembly: The wheels are turning’ (Broz, 2015).

The NOD-, LRR- and CARD-containing 4 (NLRC4, also IPAF or CARD12) is a cytosolic member of the NLR-subfamily. Its activation is depended to interaction with NAIP co-receptors (NLR-family, apoptosis inhibitory protein) able to detect PAMPs or DAMPs as, i.e. bacterial flagellin (NAIP5 and 6) (Zhao et al., 2011). Subsequently, dimerization of NLRC4-CARD with another procaspase-1 CARD initiates caspase-1 activity through self-cleavage (Latz et al., 2013). Non-active precursors of pro-inflammatory cytokines pro-IL-1ß, pro-IL-18 in proximity are then proteolytically matured into their active forms (Figure 1.2 and 1.4).

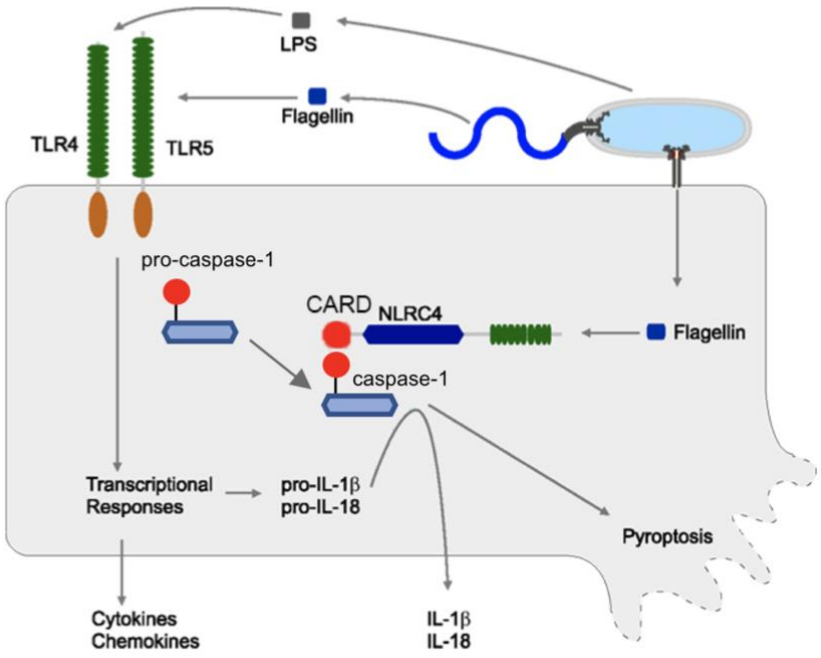

Figure 1.4: Schematic activation of caspase-1 and subsequently of IL-18 by the NLRC4 inflammasome through Flagellin/LPS stimulation. Dimer of CARD domains from NLRC4 and procaspase-1 activates inactive caspase-1 (procaspase-1), enabling processing of IL-18 precursor peptide (23kDa) into bioactive, mature IL-18 (18kDa). Adapted and modified from ‘Salmonella and caspase-1: a complex interplay of detection and evasion’ (Miao and Rajan, 2011)

1.2.5 Genetics of coronary artery disease

Single Nucleotide Polymorphisms (SNPs) are variant single base pairs within genomic DNA. Three SNP haplotypes can be distinguished: Haplotypes AA, Aa and aa. SNPs are located within both, protein-coding (exons) or non-protein-coding (introns) genes. SNPs represent approximately 90 per cent of genetic variants in the human genome and eventually regulate the function and expression of their respective gene, hence influence disease-development. Putative relevant SNPs may be identified due to genome-wide association studies (GWAS), a powerful tool for revealing associations between a common genetic polymorphism and the risk for specific disease development. For sufficient significance, data of patients, as well as healthy individuals in vast numbers, are used. Expression quantitative trait loci (eQTLs) may also be identified when implementing respective profiles of gene expression levels (Witte, 2010). Variant data within GWAS is partially determined by PCR-based genotyping but also in silico 'imputation', meaning the use of variants in linkage disequilibrium (LD, genomic proximity) to the determined SNP for statistical calculation of respective genotype (Marchini et al., 2007).

Recent GWAS meta-analyses of study-cohorts with n = up to 120.000 individuals facilitate refined tools in analysis of genetic variants (Haplotype Reference Consortium 'HRC' reference panel (Iglesias et al., 2017, Loh et al., 2016)) and confirmed 163 already known genetic variants, but also identified novel genetic loci with significant association to CAD development (Consortium et al., 2013, Kessler et al., 2013, Nikpay et al., 2015, Erdmann et al., 2018, Consortium et al., 2009). I.e. the risk for coronary artery disease is increased by 29% per risk-allele of SNP rs4977574 within the *CDKN2B-AS1* (ANRIL antisense lncRNA) gene at the *CDKN2A/B* locus at 9p21.3 (Samani et al., 2007, Kong et al., 2018). In addition to hereditary causes, various inflammatory processes were assumed to play a major role in disease pathogenesis with several immunological pathways being already described. The CANTOS trial highlighted the pro-inflammatory interleukin-1ß immunity pathway in CAD development and the relevance of inflammation itself. As described in chapter 1.2.3, experimental and clinical studies showed CAD to be more severe with increased plasma levels of pro-inflammatory IL-18. On a genetic level, prior investigations identified diverse variants within the *IL-18* loci associating with altered *IL-18* expression profiles. Another locus known was the ß-Carotene oxygenase 2 (*BCO2*) locus on chromosome 11, located in proximity to the IL-18 gene and significant association to altered IL-18

plasma levels (He et al., 2010). Moreover, independently performed GWAS looking for QTLs associated to myocardial infarction replicated the *IL-18* / *BCO 2* locus with nine significant SNPs (minimum $p = 9.36*10^{-24}$) but also identified a locus on Chr. 2 comprising several genes (*NLRC4*, *SPAST*, *MEMO1*, *DPY30*, SRD5A2, SLC30A1). Additionally, Chr. 5 showed the RAD17 locus (lead-SNP rs17229943, $p = 2.7*10^{-12}$) and Chr. 8 the MROH6 locus (lead-SNP rs2290414, $p = 1.7*10^{-17}$) (Matteini et al., 2014). Those findings on IL-18 genetics were able to be replicated in GWAS performed in 9340 patients (discovery cohort, n=3777; replication cohort, n = 5563) with the acute coronary syndrome (ACS) within the PLATelet inhibition and Patient Outcomes (PLATO) trial. Among the newly identified variants, lead-SNP rs385076 (Chr. 2: 32.489.851, GRCh37) located on Chr. 2 within the NLRC4 genes 5' untranslated region of *NLRC4* exon 2 providing the strongest association to altered IL-18 concentrations ($p = 6.99*10^{-72}$, risk allele T) (Johansson et al., 2015). The investigated NLRC4 gene extends on the short arm of Chr. 2 from base pair 32.223.625 to 32.266.682 in the region p22.3. SNP rs385076 is located at base position 2:32.264.782 in the vicinity to the CARD-coding genes. Its proxy SNP rs479333 is located at base-position 2:32.264.089 and has a linkage disequilibrium (LD) (D') = 0.823, also showing a significant association for decreased IL-18 plasma concentrations (protective allele G). The allele frequency of rs385076 protective allele T within the population was measured between 35.4% and 39.7%. As explained in chapter 1.2.4, CARD dimerization is crucial for caspase-1 activity and subsequent maturation of IL-18 and its plasma concentrations. Prior research already examined caspase-1 enzyme-activity in relation to SNP rs385076 haplotype (Eleftheriadis, 2011), but could not show a significant linkage. So far, investigations predicted a regulatory relevance but did not sufficiently explain a functional relation between *NLRC4* polymorphism rs385076 haplotype and altered levels of circulating IL-18. Detailed mechanisms on how this polymorphism, i.e. influences the interaction between the NLRC4 inflammasome and the caspase-1 activity and contributes to coronary artery disease pathogenesis, are yet not fully understood. In summary, the *NLCR4* locus on the short arm of chromosome 2 contains the most promising candidate SNPs rs385076 and its proxy SNP rs479333 for further investigations (Matteini et al., 2014, Johansson et al., 2015).

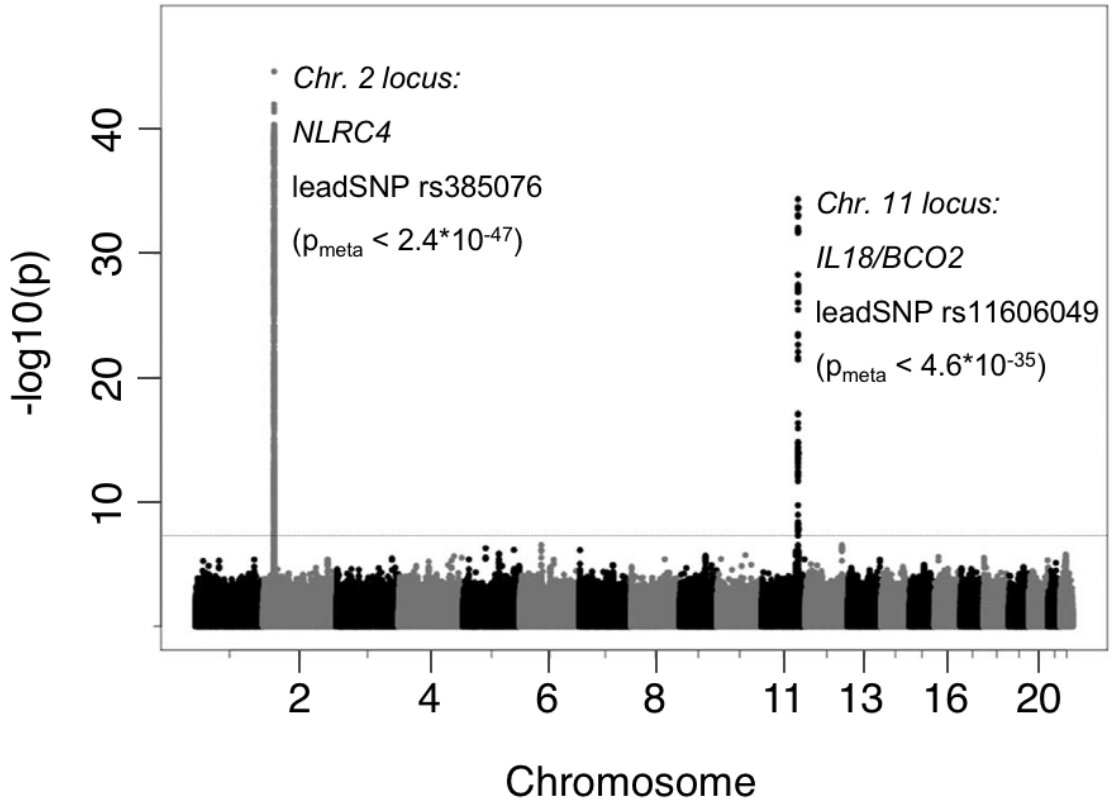

Figure 1.5: Manhattan plot of GWAS meta-analysis for IL-18 in GHS, FHS, KORA F4 and other pooled studies. Associations between allele dosage of imputed variants and log-transformed IL-18 concentration for all autosomes. Horizontal line describing genome-wide significance level ($p < 5*10^{-8}$). Adapted and modified from 'Molecular Characterization of the NLRC4 Expression in relation to Interleukin-18 Levels' (Zeller et al., 2015).

1.3 Aim of the study

Recent studies identified genetic loci with an association to IL-18 and atherosclerosis. On a molecular level, so far, the described association between genetic variants and IL-18 plasma levels has not been proofed. This thesis aimed to gain a more detailed understanding of the molecular mechanisms the known genetic variants may facilitate in the regulation of the *NLRC4* locus on chromosome 2, hence influence IL-18 concentrations and further inflammatory processes in CAD-pathogenesis. Specific aims of the thesis were:

1) Assessment of the influence of genetic variants on NLRC4 protein expression

In order to investigate the hypothesis, that NLRC4 protein level is influenced by genetic variants, the amount of NLRC4 protein in PBMCs are examined depending on the corresponding genotype of known genetic variants SNPs rs385076 (C/T) and rs479333 (G/C). The aim is, to further characterize the relationship between genetic variants and expression of NLRC4.

2) Identification of putative regulatory regions within the *NLRC4* 5'UTR region in proximity to lead SNPs

Specific untranslated regions within genes of interest may contain genetic regulatory units as transcriptional factor binding sites, hence possibly modulate post-transcriptional processes associated with their gene. In order to identify regulatory regions in the 5 ' UTR of the *NLRC4* gene, DNA fragments with different length are examined by luciferase reporter gene assay system. Furthermore, the influence of genetic variants in the *NLRC4* 5'UTR on expression (luciferase assay) is also investigated in this context.

3) Establishment of an NLRC4 qPCR model in HEK293A cells

For further investigations on the functional relation between SNPs rs385076 and rs479333 and NLRC4 protein expression, a cell-culture based model for analysing mRNA expression should be established in HEK293A cells.

2.1 Materials

2.1.1 Equipment and consumables

7900HT Fast Real-Time PCR System	Applied Biosystems, Darmstadt
Bandelin sonofication device	Bochem Laborbedarf, Bochum
DMIL LED Microscope	Leica, Wetzlar
Electrophorese chamber Mini-PROTEAN	Bio-Rad, München
Film developert CURIX 60 system	Agfa Gavaert
Incubator Heracell 150i	Thermo Fisher Scientific, Schwerte
Infinite M200 Luminometer	Tecan, Männedorf,
Nitrocellulose paper	Bio-Rad, München
Precision scale	SARTORIUS, Göttingen
Scanner Scan Maker i900	Microtek, Ratingen
Spectralphotometer Nanodrop ND-2000c	Thermo Fisher Scientific, Schwerte
Thermocycler GeneAmp PCR System 9700	Applied Biosystems, Darmstadt
Thermomixer 5436	Eppendorf, Hamburg
Transblot SD Semi-Dry Transfer Cell	Bio-Rad, München

2.1.2 Kits

QIAquick PCR Purification Kit	Qiagen, Hilden
QIAzol Lysereagents	Qiagen, Hilden
Pierce BCA Protein Assay Kit	Thermo Fisher Scientific, Schwerte
QuikChange Multi Site-Directed Mutagenesis Kit	Agilent technologies, CO, USA

2.1.3 Chemicals

Ethidium Bromide	Thermo Fisher Scientific, Schwerte
100x bovine serum albumin (BSA)	Bio-Rad, München
Deoxynucleotide (dNTP) Solution Mix	New England Biolabs, Frankfurt
Dimethyl sulfoxide (DMSO)	Merck, Darmstadt
EDTA	Sigma-Aldrich, MO, USA
Glacial acetic acid	Sigma-Aldrich, MO, USA
Agarose	Sigma-Aldrich, MO, USA
Acrylamid (40%)	Roth, Karlsruhe
APS (10%)	Roth, Karlsruhe
Tween 20	Sigma-Aldrich, MO, USA
TEMED	Roth, Karlsruhe
SDS	Roth, Karlsruhe
Aqua dist.	Braun, Melsungen
ECL Plus	GE Healthcare, München
Ethanol	AppliChem, Darmstadt
Glycin	Roth, Karlsruhe
Milk powder	Bio-Rad, München

2.1.4 Buffers

Laemmli	Sigma-Aldrich, MO, USA

Tris-borate-EDTA (TBE, 10x)

Reagent	*Volume/Mass*
Tris Base	54 g
Boric acid	27.5 g
0.5 M EDTA (pH 8.0)	20 ml
Distilled H_2O	1000 ml

Loading buffer (pH = 6.8)

Reagent	*Volume/Mass*
Millipore-H_2O	1000 ml
Tris	60.6 g
EDTA	3 g
SDS	4 g

pH-adjustment to pH = 8.8 with HCl

Resolving buffer (pH = 8.8)

Reagent	*Volume/Mass*
Millipore-H_2O	1000 ml
Tris	181.7 g
EDTA	3 g
SDS	4 g

pH-adjustment to pH = 6.8 with HCl

2.1.5 Enzymes, enzyme-buffers, etc.

Gel Loading Dye blue	New England Biolabs, Frankfurt
KpnI	Fermentas GmbH, St. Leon-Rot
Lipofectamine 2000	Thermo Fisher Scientific, Schwerte
Molecular Weight Ladder (100bp-1000bp)	New England Biolabs, Frankfurt
NEBuffer 2 (10x)	New England Biolabs, Frankfurt
NEBuffer 4 (10x)	New England Biolabs, Frankfurt
NheI	Fermentas GmbH, St. Leon-Rot
PageRuler Unstained/Prestained	Thermo Fisher Scientific, Schwerte
Phusion® HF Buffer (5x)	New England Biolabs, Frankfurt
Phusion® HF DNA polymerase	New England Biolabs, Frankfurt
T4 DNA Ligase Reaction Buffer (10x)	New England Biolabs, Frankfurt
T4 DNA-Ligase	New England Biolabs, Frankfurt

2.1.6 Cell culture growth medium

Dulbecco's Modified Eagle Medium (DMEM) + 4,5g/l D-Glucose	Biochrom, Berlin
Opti-MEM (reduced serum medium)	Thermo Fisher scientific, Schwerte

Lysogny broth (LB)-Luria Medium

Reagent	*Volume/Mass*
Yeast extract	5 g
Trypton	10 g
NaCl	0,5 g
Distilled H_2O	1 l

Super optimal Broth transformation (SOC) Medium

Reagent	*Volume/Mass*
Tryptane	4 g
Yeast extract	1 g
NaCl	0.12 g
KCl	0.04 g
$MgCl_2$	0.8 g
$MgSO_4$	0.5 g
Distilled H_2O	200 ml
D-Glucose	20 mM

2.1.7 Antibiotics

Penicillin 100 U/l	Sigma-Aldrich, MO, USA
Streptomycin 100µg/ml	Sigma-Aldrich, MO, USA

2.1.8 Antibodies	Target	Host	
Primary antibody	anti-CLAN Protein (CARD12/NLRC4)	Rabbit	Sigma-Aldrich, MO, USA
Secondary antibody	anti-Actin	Rabbit	Sigma-Aldrich, MO, USA

2.1.9 Reporter gene assay

Steady Glo Luciferase assay	Promega, WI, USA

2.1.10 Plasmids

pGL4.10 [luc2]	Genbank AY738222	Promega, WI, USA
pGL4.23 [luc2/minP]	Genbank DQ904455	Promega, WI, USA
pEYFP		CloneTech / Takara Bio Europe, St-Germain-en-Laye, France
pDRIVE		Qiagen, Hilden

2.1.11 Mini-Preparation solutions

Solution 1

(4°C storage, no autoclavation)

Reagent	*Volume/Mass*
Glucose	50 mM (5 ml, 1M)
Tris	25 mM (2.5 ml, 1M, pH = 8)
EDTA	10 mM (2 ml, 0.5 M, pH = 8)
Distilled H_2O	Up to 100 ml

Solution 2

(fresh preparation, no autoclavation)

Reagent	*Volume/Mass*
NaOH	0.2 M, 5 ml 2N NaOH
SDS 1%	5 ml, SDS 10%
Distilled H_2O	Up to 50 ml

Solution 3

(autoclavation)

Reagent	*Volume/Mass*
NaAc-Trihyd	5 M, 40.9g in 40 ml dist. H_2O + X up to 60 ml
Concentrated acetic acid	11.5 ml
Distilled H_2O	Up to 100 ml

2.1.12 Oligonucleotides

Table 2.1.12.1: Details on oligonucleotides of TaqMan® Pre-designed SNP rs385076 Genotyping (Assay ID: C___3207332_10; Thermo Fisher Scientific, Schwerte)

Description	**Sequence 5' – 3'**	**Detector**
SNP allele(normal) rs385076(C)	GCCCTCTTCTTGGGAGACCAAGACA**[C]**GTTTTTAAAAT AAAGTTTCTTTGTA	VIC
SNP allele(IL18+) rs385076(T)	GCCCTCTTCTTGGGAGACCAAGACA**[T]**GTTTTTAAAAT AAAGTTTCTTTGTA	FAM

Table 2.1.12.2: Details on oligonucleotides primers of self-produced TaqMan® SNP Genotyping Assays, rs479333.

Description	Sequence 5' – 3'	Detector
SNP allele(normal) rs479333(G)	ATTGGATGGACTAAGTAGTCCACCT**[G]**GTTCCTTTCAG CTTTGATCATCTGT	VIC
SNP allele(IL18+) rs479333(C)	ATTGGATGGACTAAGTAGTCCACCT**[C]**GTTCCTTTCAG CTTTGATCATCTGT	FAM

Table 2.1.12.3: Details on oligonucleotide primers for reporter gene assay amplicons.

Description	Sequence 5' – 3'	Restriction site
Forward 1	CTT**[GGTAC|C]**TCCAATCTCCCAAGTTACTGA	KpnI
Forward 2	GCATTACAGAAA**[GGTAC|C]**TCACTCTTTTTT	KpnI
Forward 3	TGCCCTCCAGCTTG**[GGTAC|C]**AGAACAAGAC	KpnI
Reverse 1	TGTT**[G|CTAGC]**ACCCAGTCTATGGTATTTTA	NheI
Reverse 2	TAGCTGGGGCGCGGTGCCC**[G|CTAGC]**TGTAA	NheI

Table 2.1.12.4: Details on oligonucleotide amplicons for reporter gene assay (whole sequence).

Amplicon	NLRC4 5' exon 2 - 5'UTR (Sequence 5' – 3')
Upstream 318 nt	**Primer Reverse 1** **CACCCAGTCTATGGTATTTTA**AACACATTAATACGACTAATATTATAAAAGTGTGTG AACAGTTAAGAAGTGTGCTGACCAGGTTCTATCCTAGTTTTGTAGACAATTAGCAGT GTGATGTAGGGCAGGACATTTAACTCCTCTCTACCACATTTTCCACCTCTCAAAGCC AGGCTGCAAGGATCTACTGAGATAATGTACATAAAGACCCTATCACGAAATAGGTGT CCCGTAAAGGGTGATTTCCTTCACTTCTGTCTCCAAATATCAGGTTTCTCA**TCAGTA** **ACTTGGGAGATTGGA** **Primer Forward 1**
	Locus chromosome 2:32.488.839 - 32.489.138 (GRCh37)

Amplicon	NLRC4 5’ exon 2 - 5’UTR (Sequence 5’ – 3’)

rs479333 (IL18+)

rs479333 (0)

716 nt

Primer Reverse 1

CACCCAGTCTATGGTATTTTAAACACATTAATACGACTAATATTATAAAAGTGTGTG
AACAGTTAAGAAGTGTGCTGACCAGGTTCTATCCTAGTTTTGTAGACAATTAGCAGT
GTGATGTAGGGCAGGACATTTAACTCCTCTCTACCACATTTTCCACCTCTCAAAGCC
AGGCTGCAAGGATCTACTGAGATAATGTACATAAAGACCCTATCACGAAATAGGTGT
CCCGTAAAGGGTGATTTCCTTCACTTCTGTCTCCAAATATCAGGTTTCTCATCAGTA
ACTTGGGAGATTGGATGGACTAAGTAGTCCACCT**[C|G]**GTTCCTTTCAGCTTTGAT
CATCTGTGATTCTAACAACAGTCTTAGCAACAAGAGTGAGTTTCCTGGCCGGGCACG
TTGGCTCACACCTGTAATCCCAGCACTTTGGGAGGCTGAGGTGGGCAGATCACGAGG
TCAGGAGTTGAGACCAGTCTGGCCAACATGGTGAAACCCTGTCTCTACTAAAAATAC
AAAAATTAGCTGGGGCGCGGTGCCGGGTGCCTGTAATCCCAGCTACTTGGGAGGCTG
AGGCAGGAGAATTGCTTGAACCCAGGAGGCAGAGGTTGCAGTGAGCCGAGATCACGC
CACTGCAGTCCAGCCTGGGTGACAGAGCAAGACTCTGTCTCAAAAAAAAAAAAA**AAA**
AAAGAGTGAG
Primer Forward 2

Locus chromosome	2:32.488.839 - 32.489.528 (GRCh37)
SNP rs479333	2:32.489.158 (GRCh37)

both (IL18+)

both (0)

1476 nt

Primer Reverse 1

CACCCAGTCTATGGTATTTTAAACACATTAATACGACTAAATTATAAAAGTGTGTGA
ACAGTTAAGAAGTGTGCTGACCAGGTTCTATCCTAGTTTTGTAGACAATTAGCAGTG
TGATGTAGGGCAGGACATTTAACTCCTCTCTACCACATTTTCCACCTCTCAAAGCCA
GGCTGCAAGGATCTACTGAGATAATGTACATAAAGACCCTATCACGAAATAGGTGTC
CCGTAAAGGGTGATTTCCTTCACTTCTGTCTCCAAATATCAGGTTTCTCATCAGTAA
CTTGGGAGATTGGATGGACTAAGTAGTCCACCT**[C|G]**GTTCCTTTCAGCTTTGATC
ATCTGTGATTCTAACAACAGTCTTAGCAACAAGAGTGAGTTTCCTGGCCGGGCACGT
TGGCTCACACCTGTAATCCCAGCACTTTGGGAGGCTGAGGTGGGCAGATCACGAGGT
CAGGAGTTGAGACCAGTCTGGCCAACATGGTGAAACCCTGTCTCTACTAAAAATACA
AAAATTAGCTGGGGCGCGGTGCCGGGTGCCTGTAATCCCAGCTACTTGGGAGGCTGA
GGCAGGAGAATTGCTTGAACCCAGGAGGCAGAGGTTGCAGTGAGCCGAGATCACGCC
ACTGCAGTCCAGCCTGGGTGACAGAGCAAGACTCTGTCTCAAAAAAAAAAAAAAAAA
AAGAGTGAGTTTCCTTTCTGTAATGCCAAAAAGTGTTTCCAAAGTCCTTTCCATCTC
ACAGTAGTCCAAGGGGTACATGTACCCCTTGAACCTGATGAAGCCCCAGCAGACCCG
ATTAACCACCCCTAAAGGTTTCTCGGCAGGCAAATCCAGCCAGGCATGCAAATCACA
CTCGTCAATGTTAAGGCTTTTGTACATCCCAGACACAAGCTTTAAATGAATGTAAAC
CCAGATTTTAATATTTGGGCCCCAGACCTTAAAAATCCCATTCTCTCTACCCACAGT
ACCTGGCTGAGCAATCCAATTGCCCTCTTCTTGGGAGACCAAGACA**[T|C]**GTTTTT
AAAATAAAGTTTCTTTGTATTTGCTTTCCGTTTCAGTGAGGCCTCGAGTTCTTGTAG
ACCAGATACCTTCTTGTTCTGTGAGAGGACAGTGTACAGAGAGGGGAACTGCTGAGC
AGTTCCTTTTTTTTTTTTCAAAGCACAGTAAGAGTGGTTTGGACACAAGTACTACCA
GTTCAGAAAGGGAAGATGGGTGTAGGCAGGAGTAGCCGGGGAAGAAGTAGAACTTCA
GAGTAAAAGATGCAAGAGCTAGAAATTCCGTCAAGAAAGGAATTACTCATTTGTTTC
CTGTTTGTTCACAACATATGAATTCATTGCTGTTGAGTTACTTATTCTATACCTTAA
AATGAAACAAAGTCTTCTGAACATCCAACATATATTTTTTTCTTTTTCTTTCTTTT
TTCTTTTTTTTGAGACAGA**GTCTTGTTCTG**
Primer Forward 3

Locus chromosome	2:32.488.839 - 32.490.286 (GRCh37)
SNP rs479333	2:32.489.158 (GRCh37)
SNP rs385076	2:32.489.851 (GRCh37)

rs385076 (IL18+)

rs385076 (0)

952 nt

Primer Reverse 2

CTGTAATCCCAGCTACTTGGGAGGCTGAGGCAGGAGAATTGCTTGAACCCAGGAGG
CAGAGGTTGCAGTGAGCCGAGATCACGCCACTGCAGTCCAGCCTGGGTGACAGAGC
AAGACTCTGTCTCAAAAAAAAAAAAAAAAAAAGAGTGAGTTTCCTTTCTGTAATGC
CAAAAAGTGTTTCCAAAGTCCTTTCCATCTCACAGTAGTCCAAGGGGTACATGTAC
CCCTTGAACCTGATGAAGCCCCAGCAGACCCGATTAACCACCCCTAAAGGTTTCTC
GGCAGGCAAATCCAGCCAGGCATGCAAATCACACTCGTCAATGTTAAGGCTTTTGT
ACATCCCAGACACAAGCTTTAAATGAATGTAAACCCAGATTTTAATATTTGGGCCC
CAGACCTTAAAAATCCCATTCTCTCTACCCACAGTACCTGGCTGAGCAATCCAATT
GCCCTCTTCTTGGGAGACCAAGACA**[T|C]**GTTTTTAAAATAAAGTTTCTTTGTAT
TTGCTTTCCGTTTCAGTGAGGCCTCGAGTTCTTGTAGACCAGATACCTTCTTGTTC
TGTGAGAGGACAGTGTACAGAGAGGGGAACTGCTGAGCAGTTCCTTTTTTTTTTT
CAAAGCACAGTAAGAGTGGTTTGGACACAAGTACTACCAGTTCAGAAAGGGAAGAT
GGGTGTAGGCAGGAGTAGCCGGGGAAGAAGTAGAACTTCAGAGTAAAAGATGCAAG
AGCTAGAAATTCCGTCAAGAAAGGAATTACTCATTTGTTTCCTGTTTGTTCACAAC
ATATGAATTCATTGCTGTTGAGTTACTTATTCTATACCTTAAAATGAAACAAAGTC
TTCTGAACATCCAACATATATTTTTTTCTTTTTCTTTCTTTTTTCTTTTTTTTGA
GACAGA**GTCTTGTTCTG**

Primer Forward 3

Locus chromosome	2:32.489.378 - 32.490.286 (GRCh37)
SNP rs385076	2:32.489.851 (GRCh37)

Table 2.1.12.5: Details on oligonucleotide primers for site-directed mutagenesis.

Description	Sequence 5' – 3'	Allele
rs385076 Forward	CTTTATTTTAAAAAC**[G]**TGTCTTGGTCTCCC	C
rs385076 Reverse	GGGAGACCAAGACA**[C]**GTTTTTAAAATAAAG	C
rs479333 Forward	CAAAGCTGAAAGGAAC**[C]**AGGTGGACTACTTA	G
rs479333 Reverse	TAAGTAGTCCACCT**[G]**GTTCCTTTCAGCTTTG	G

2.2 Methods

2.2.1 Genotyping

Genotyping examines differences in genotypes, i.e. highly divergent gene areas such as SNPs or microsatellites. Using fluorescence and polymerase chain reaction (Real-Time TaqMan® PCR Technology), specific gene sequences are compared with reference sequences, thus inherited alleles of the examined samples are determined. Genotyping allele configuration of SNPs rs385076 and rs479333 was performed using TaqMan® genotyping assays according to the protocol for TaqMan® SNP (Applied Biosystems). TaqMan® method uses polymerases 5' nuclease activity in a polymerase chain reaction (PCR, see 2.2.2.5) and oligonucleotide-probes complementary to the examined gene region. Real-time PCR (ABI Real-time PCR 7900 HT System; q-RT-PCR, see 2.2.2.11) system was used for investigations on SNPs mentioned above. Each Oligonucleotide-probe binds exactly to either one or the other SNP allele with specific affinity and contains a fluorescent reporter dye (e.g. FAM or VIC, also 6-carboxyflourescein) on its 5' end matching the respective allele. Quencher dye (e.g. TAMRA, 6-carboxy-tetramethyl-rhodamine) is attached to its 3' end.

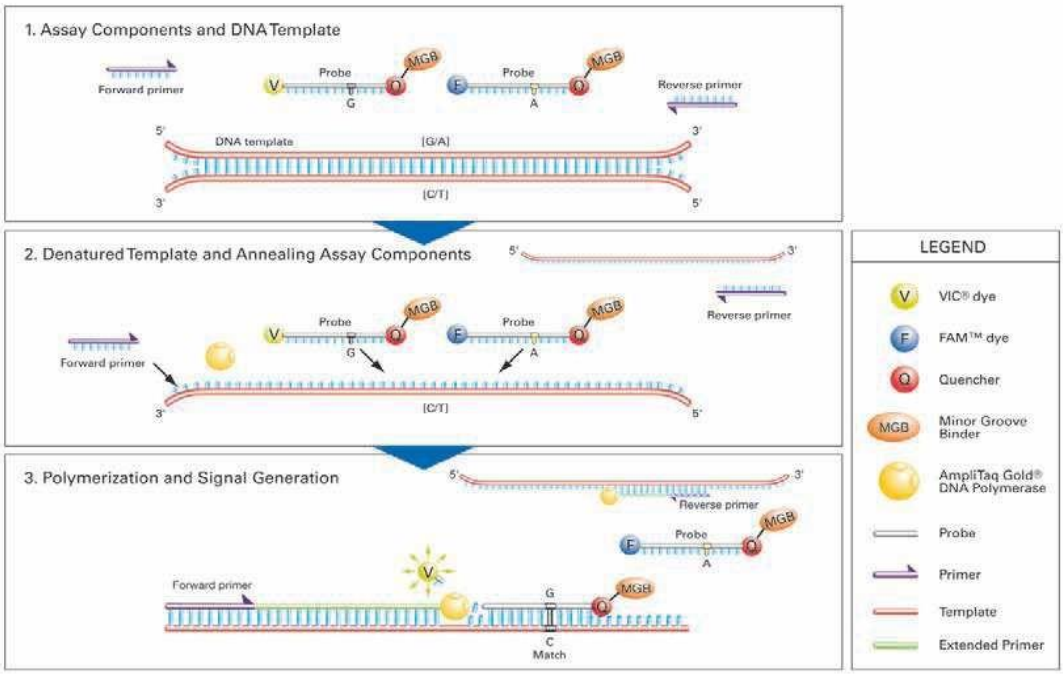

Figure 2.1: Principle of TaqMan® q-RT-PCR. Modified figure by Applied Biosystems, TaqMan® Genotyping Assay. 1. Overview of necessary agents for TaqMan® q-RT-PCR or

SNP genotyping. Increased temperature leads to cDNA denaturation. No fluorescent light is emitted due to the minor groove binder (MGB) quencher.
2. The temperature is lowered, so the primers and oligonucleotides can anneal to their matching sequence on the DNA strands.
3. The complementary DNA strand is polymerised. The DNA polymerase thereby separates the quencher from the fluorescent dye. The now emitted signals can be associated with expression profiles or genotypes. Adapted and modified from TaqMan® Applied Biosystems reference guide (AppliedBiosystems, 2019a).

During polymerisation, fluorescent signals are produced when Taq-polymerase enzyme cleaves the DNA-bound probe, thus activating the respective fluorophores by untightening the vicinity of their quencher (see figure 2.1). Signals are then interpreted by a detection software fitted to the q-RT-PCR system. To be determined SNP rs385076 requires pre-designed and pre-mixed TaqMan® (5' nuclease) SNP Genotyping Assay as well as TaqMan® Genotyping Master Mix providing necessary primers and probes. TaqMan® genotyping assay for rs479333 is mixed individually according to Table 2.2.3. The DNA-amount used within runs is 10ng per sample, non-template controls (NTCs) were included for quality control. Preparation of samples is done according to Table 2.2.2 and 2.2.3 and distributed into 96-well-plates. Short centrifugation is applied for 1 min at 1000 *rpm*. Prior to PCR, the baseline intensity of the fluorophores is quantified. PCR is carried out on GeneAmp 9700 Thermocycler according to program in Table 2.2.1. Subsequently, plate read is done immediately after PCR cycles. The detection software analyses fluorescence signal of each well individually and aligns noted colour-value with the corresponding allele. Homozygosity for each of the alleles is determined by fluorescence of, e.g. either FAM or VIC dye. Detection of both fluorescent signals indicates heterozygosity of allele configuration. Negative signals are either control samples or indicate an insufficient amount of, i.e. DNA. Genotyping results are also displayed as scatter plots and checked through TaqMan® automated allele determination with confidence interval set to 95%.

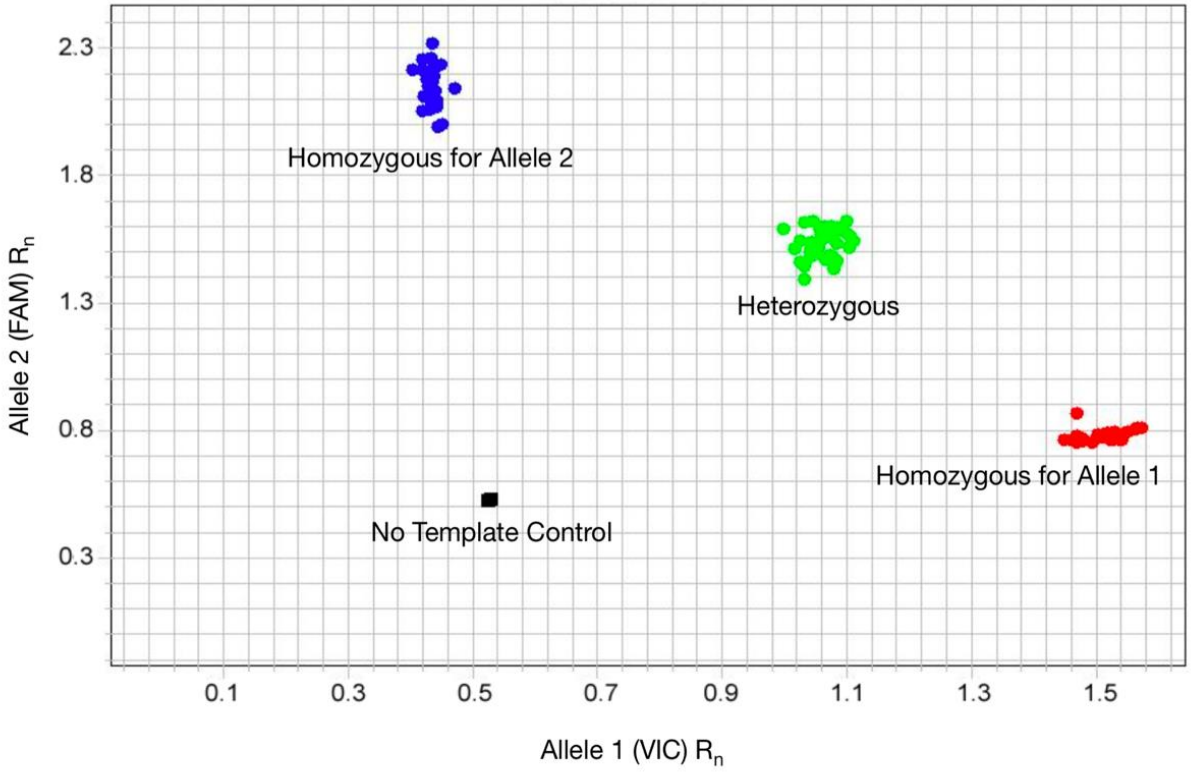

Figure 2.2: A three-cluster allelic discrimination plot generated with TaqMan® SNP Genotyping Assay. Samples are represented as dots and aligned either with x- or y-axis according to their homozygous allele configuration. Samples with heterozygous allele configuration of investigated SNPs are clustered in the top right corner. Adapted and modified figure by Applied Biosystems, TaqMan® Genotyping User Guide (AppliedBiosystems, 2019b).

Table 2.2.1: Details on thermocycler program for DNA-amplification.

Step	Temperature	Time	Cycles
Denaturation	95 °C	10 minutes	
Annealing	92 °C	15 seconds	40 - 50x
Elongation	66 °C	1 minutes	
Hold	4 °C	∞	

Table 2.2.2: Details on pre-designed TaqMan® SNP Genotyping Assay master mix, 7µl per sample/well for SNP rs385076 (T/C).

Reagent	Volume/Mass
TaqMan® SNP Genotyping Assay (20x)	0,35 µl
DNA (20 [ng/µl])	0.5 µl
Buffer (2x)	3.5 µl
DNAse-free H_2O	Up to 7 µl

Table 2.2.3: Details on self-produced TaqMan® SNP Genotyping Assay master mix; 7µl per sample/well for SNP rs479333(C/G).

Reagent		Final concentration
Forward Primer	rs479333F	0.9 [pmol/µl]
Reverse Primer	rs479333R	0.9 [pmol/µl]
SNP allele (IL18+)	rs479333G	0.2 [pmol/µl]
SNP allele (normal)	rs479333C	0.2 [pmol/µl]
	dNTP	10 [mM]
Biotaq DNA Polymerase (Bioline®)		5 [U/µl]
	Rox (50x)	1x
	$MgCl_2$	5.0 [mM]
	NH_4 Buffer (10x)	1x
	DNA (20 [ng/µl])	20 [ng/µl])
	DNAse-free H_2O	

For details on genotyping primer sequences see, Table 2.1.12.1 and 2.1.12.2.

2.2.2 Protein and biochemical methods

2.2.2.1 Protein quantification

Total protein concentration is determined using the Pierce BCA Protein Assay Kit (Thermo Scientific, Schwerte). This method is based on the biuret reaction, i.e. the reduction of copper cations by proteins in an alkaline medium. In the presence of BCA (bicinchoninic acid), copper cations form a complex which has a high light absorption linear to the protein content of the measurement solution. Bovine serum albumin (BSA) is used to generate a standard curve (25 µg / ml- 2000 µg / ml) to calculate the unknown protein content of protein lysates using linear regression analysis. 25 µl of BSA standard or sample are incubated on a 96-well plate (Bio-Rad, Munich) with 200 µl Working Reagent of the kit per well for 30 min at 37°C. The absorbance of all samples on the plate then is measured within 10 min photometrical at 562 nm wavelength.

2.2.2.2 Western Blot

Western Blot protein quantification was used to determine NLRC4 protein levels in protein lysate samples from GHS individuals.

SDS-Polyacrylamide gel electrophoresis

Gel electrophoresis is performed with 10% SDS acrylamide gels (table 2.2.4 and 2.2.5). Wells are loaded with each 20µg protein lysate + 4 µl Lämmli (1:1) loading buffer (Laemmli, 1970). Each gel is loaded with up to 12 lysates and further given a batch number. Protein lysate samples are denatured at 95°C for 3 min before loading. First and last well are loaded with Benchmark Prestained Markers (Thermo Fisher Scientific, Schwerte). The combined time for protein migration and -separation is 75 minutes at 120 V.

Protein transfer (Semi-Dry Western Blotting)

The electrophoretic wet-blot method with sandwich technique is used to transfer proteins to a 0.2 µm nitrocellulose membrane at 100 mA/h for 1.5 h. Uniform protein transfer is controlled by staining with Ponceau S according to Montelaro (Salinovich & Montelaro 1986) and destained with 1x TBST buffer (see material). Membranes are blocked with 5% skimmed milk in 1x TBST by overnight incubation at 4°C. The primary antibody is applied in a solution of 5% skimmed milk with 1x TBST (concentration in final solution [c = 1:1.000]) for 1.5 hours at room temperature, followed by three times

10 minutes washing with 1x TBST. Application of secondary antibody in an equal solution (concentration in final solution [c = 1:10.000]) is made for 1-hour at room temperature, again followed by similar washing with 1x TBST. Details on antibodies can be found in table 2.1.8.

Chemiluminescence and image development

Detection of stained proteins using antibody complexes is performed with a Chemiluminescence system (ECL Plus, GE Healthcare Europe GmbH, Munich) and documented on X-ray film (CURIX 60 system, Agfa Gevaert). Membrane proteins are quantified with ImageJ Java-based imaging system (National Institute of Health, U.S. Department of Health and Human Services). The normalisation of respective density values for NLRC4 protein was done with an antibody addressing actin as reference protein (housekeeper), invariances between batches are analysed and adjusted statistically.

Table 2.2.4: Composition of loading gel (pair, 4.5%) used for SDS-Page (10%) blotting.

Reagent	Volume/Mass
Destilled H_2O	6.4 ml
Loading buffer pH 6.8	2.5 ml
Acrylamid/bisacrylamid 40%	1.1 ml
TEMED	35 µl
APS 10%	100 µl

Table 2.2.5: Composition of resolving gel (pair, 10%) used for SDS-Page (10%) blotting.

Reagent	Volume/Mass
Destilled H_2O	10 ml
Resolving buffer pH 8,8	5 ml
Acrylamid/bisacrylamid 40%	5 ml
TEMED	35 µl
APS 10%	100 µl

2.2.2.3 Agarose-gel electrophoresis of PCR products

Gel electrophoresis technique is used for the separation of DNA fragments. Under the influence of electric current DNA fragments move within the agarose-gel in relation to their length and respective electric charges. DNA fragments are analysed in 1% agarose gel according to the table below. Samples of DNA fragments are mixed with Loading Dye. Additionally, NEB DNA ladders (100bp – 1kbp) are loaded into the first and last well of the gel. Running buffer used for electrophoresis is TBE (1x) with a runtime of 2 hours at 80 V. Following documentation is done with a CCD video camera.

Table 2.2.6: Details on agarose gel (1%) composition.

Reagent	Volume/Mass
Agarose	1 g
TRIS-Borat-EDTA buffer (TBE) 1x	100 ml
Ethidium-bromid 87 (into the liquid gel)	6 µl

2.2.2.4 Purification of DNA Fragments from agarose gel

Excised oligonucleotides are purified using QIAquick Gel Extraction Kit (Qiagen, Hilden) according to its user manual. Purified PCR products are eluted in 20-50 µl nuclease-free H_2O.

2.2.2.5 Polymerase Chain Reaction (PCR)

Polymerase chain reaction (PCR) is used to replicate genetic material like DNA identically to its original sample using specific enzymes. DNA fragments used within the experiments are amplified utilising PCR, primers specific to the investigated gene were pre-designed by prior investigators. The first amplicon to be synthesized is ‘both (IL18+)’ and used as template DNA for remaining ones. Preparation of reaction mixture and settings for thermocycler are done according to Table 2.2.7 and 2.2.8.

Table 2.2.7: Details on PCR reagent mixture for 40µl reaction mastermix.

Reagents	Volume/Mass
Phusion Polymerase (F-530L; NEB, 2U/µl)	0.4 µl
10mM dNTPs	0.8 µl
Phusion Buffer GC (5x)	8 µl
DMSO	1.2 µl
Forward Primer	0.5 µM
Reverse Primer	0.5 µM
Template DNA (100 ng/µl)	0,5 µl
Nuclease free H_2O	Remaining volume up to 40 µl

Table 2.2.8: Details on thermocycler program for amplification of amplicon 'both (IL18+)' and 'both (0)'.

Step	Temperature	Time	Cycles
Enzyme activation	94 °C	1 minutes	1x
Denaturation	94 °C	10 seconds	40 x
Annealing	55 °C	30 seconds	
Elongation	72 °C	1 minutes	
Final elongation	72 °C	10 minutes	1x
Hold	4 °C	∞	

2.2.2.6 Photometric quantification of nucleic acid

Photometric measurements determine the concentration of nucleic acids with Nanodrop ND-2000c photometer (Thermo Fisher Scientific, Schwerte). Nucleic acid samples in a ratio of 1:50 to 1:100 are measured with UV light absorption at a wavelength of 260 nm and 280 nm. For consecutive purity check-up samples with calculated ratio (260 nm/280 nm) greater than 1.8 and less than 2.1 are considered not contaminated by organic components/proteins and submitted for further dilution to the desired concentration.

2.2.2.7 Enzymatic restriction of plasmid DNA and oligonucleotides

The enzymatic restriction is a targeted, enzymatic division of oligonucleotides employing endonucleases targeting defined base-sequences. Resulting DNA fragments may either be analysed by their sizes (comparative analysis of fragments) or further prepared for DNA cloning. Restrictive digestion is performed according to Table 2.2.9 below. The master mix with 200 ng DNA is incubated for 30 minutes at 37°C. After enzymatic restriction, samples are separated through agarose gel electrophoresis (see chapter 2.2.4.2) and purified by QIAGEN PCR Purification kit according to the user manual.

Table 2.2.9: Details on enzymatic restriction of plasmid DNA and oligonucleotides; 10 µl reaction-mix.

Reagent	Volume/Mass
Restrictive enzyme (10 U/µl)	0.3 µl
Enzyme buffer	1.0 µl
BSA (10x)	1 µl
DNA [100 ng/µl]	2.0 µl
Distilled H_2O	up to 10 µl

2.2.2.8 Enzymatic ligation of linearized plasmid DNA and oligonucleotides

DNA ligation is an enzyme-catalysed linkage of two non-circular segments at their ends. A phosphodiester bond is established between the 3'-hydroxy end of one segment to the 5'-phosphate end of the other nucleic acid segment. Generated amplicon and plasmid DNA are prepared for ligation by digestive restriction (see chapter 2.2.2.7). Ligation reaction master mix with 100 ng purified PCR product per reaction is carried out overnight in a 16°C tempered water bath according to the user-manual and the following table:

Table 2.2.10: Details on T4-Ligation reaction-mix.

Reagent	Volume/Mass
Vector (25 ng)	0.5 µl
Amplicon (100 ng)	1 µl
Ligation Master Mix (2x)	5 µl
Distilled H_2O	up to 10 µl

2.2.2.9 DNA sequencing

The DNA sequencing was carried out at the company GATC-Biotech (Konstanz, https://www.gatc-biotech.com). For this purpose, samples of 300 ng DNA and 1 pmol sequencing primers are brought to a total volume of 10 µl with nuclease-free water and send to the company mentioned above.

2.2.2.10 Reverse transcriptase PCR for cDNA amplification

To assess the general NLRC4 gene expression in HEK293A and the effect of LPS stimulation, cDNA is generated from respective RNA samples to perform quantitative analysis of the gene-expression using quantitative real-time PCR (qPCR). High Capacity cDNA Reverse Transcription Kit (Applied Biosystems, Darmstadt) is used according to the user manual.

Table 2.2.11: Details on *NLRC4* reverse transcription reagent mixture for 10 µl/reaction.

Reagent	Volume/Mass
MultiScribe™ Reverse Transcriptase	0.5 µl
RT Buffer (10x)	1.0 µl
dNTP Mix (100 mM, 25x)	0.4 µl
RT Random Primers (10x)	1.0 µl
RNA-sample c = [25 ng/µl]	2.0 µl
Nuclease-free H_2O	5.1 µl

Table 2.2.12: Details on thermocycler program for *NLCR4* RNA reverse transcription.

Step	Temperature	Time
Annealing	25°C	10 minutes
Rewriting	37°C	2 hours
Hold	4°C	∞

2.2.2.11 Quantitative polymerase chain reaction (qPCR)

The quantitative real-time PCR (qPCR) is a PCR method in which PCR products can be quantified by measurement of fluorescence emitted by specific dyes during the exponential phase of the PCR. The fluorescence-emission is proportional to the number of PCR-products; thus, quantification of amplicons is immediately possible and also illustrated by the qPCR polycycler. The PCR is carried out on a 7900HT Fast Real-Time PCR System. *NLCR4* gene transcription of untreated HEK293A cells, as well as LPS stimulated HEK293A cells (*NLRC4* overexpression), are evaluated by using qPCR with over 40 cycles and respective cDNA (see 2.2.2.10) with either 5, 10 or 22,5ng cDNA within each sample. *NLRC4* gene expression is normalised with GAPDH expression and evaluated by Ct values (threshold cycle value, fluorescence signal increases significantly above the background fluorescence) with the calculation of Δ Ct of Ct *NLRC4* - Ct GAPDH.

Table 2.2.13: Details on *NLRC4* qPCR reagent mixture for 10 µl/reaction.

Reagent	Volume/Mass
TaqMan® Gene Expression assay (20x forward/reverse primers, probes)	0.5 µl
cDNA [100 ng/ul]	1 µl
TaqMan® Gene Expression assay mastermix	5 µl
nuclease-free H_2O	3.5 µl

Table 2.2.14: Details on thermocycler program for *NLCR4* qPCR on cDNA of untreated and LPS stimulated HEK293A cells.

Step	Temperature	Time	Cycles
Enzyme activation	95°C	10 minutes	1 x
Denaturation	95°C	15 seconds	40 x
Annealing	60°C	1 minute	
Extension	60°C		
Hold	4°C	∞	

2.2.2.12 Site-directed mutagenesis (Ligation-During-Amplification 'LDA')

Site-directed mutagenesis allows the modification of DNA by recombinant oligonucleotides, i.e. the exchange of individual nucleobases of a gene in a targeted manner. Mutagenic primers and template DNA (circular plasmid DNA) are linearly amplified and ligated in several cycles using a thermocycler. QuikChange Multi Site-Directed Mutagenesis Kit (Agilent technologies, CO, USA) is used according to the instruction manual.

Table 2.2.15: Reagents for 50 µl QuickChange site-directed mutagenesis PCR reaction mastermix.

Reagents	Volume/Mass
Reaction Buffer	5 µl
Amplicon DNA (1 ng/ul)	10 µl
Forward primer (10 µM)	1.25 µl
Reverse primer (10 µM)	1.25 µl
dNTP mix	1 µl
QuickSolution	3 µl
PfuTurbo Polymerase	1 µl
Destilled H_2O	27.5 µl

Table 2.2.16: Details on thermocycler program for QuikChange site-directed mutagenesis PCR.

Step	Temperature	Time	Cycles
Enzyme activation	95°C	1 minute	1 x
Denaturation	95°C	50 seconds	**18 x**
Annealing	60°C	50 seconds	
Extension	68°C	5 minutes	
Final Extension	68°C	1 minute	1 x
Hold	37°C	∞	

2.2.3 Cell culture

2.2.3.1 Cultivation of Human Embryonic Kidney cells 293A (HEK293A)

Human embryonic kidney 293A (HEK293A) cells are used in cell culture experiments. Cultivation is done at 37°C with H_2O-saturated atmosphere of 95% containing 5% CO_2. Cells are cultivated in Dulbecco's Modified Eagle Medium (DMEM, infused with 10% FCS and 1% penicillin/streptomycin, see materials). Supplement for used medium consisting of 10% fetal calf serum plus 1% Penicillin/Streptomycin (10.000 U/ml/10.000 µg/ml). Change of DMEM growth medium is done twice per week, whereas passage and splitting of the cells are performed at confluency = 70-90%. Prior to transfection, a stable cell count is insured by using a Neubauer counting chamber. Cells in suspension are counted in the chamber under light microscopy. For calculation, the cell count of all four corner squares is used with the following formula:

(Cell count in all four corner squares) x 2.5 x 10^3 = Number of cells/ml

2.2.3.2 Cryopreservation of HEK293A cells

For long-term storage cells of a 75 ml bottle are trypsinized, centrifuged and the supernatant is discarded. The resulting cell pellet is resuspended in 500 µl of freezing medium (FCS + 10% DMSO) and cooled to -80 ° C in cryogenic tubes at about 1°C/min. Cells in cryotubes may temporally be stored at -80°C, but transferred into liquid N_2 for longer storage. Recultivation is performed by rapid defrosting of cryotubes

in a 37°C water bath and resuspension of cells in DMEM. DMSO residues are removed by medium change after attachment of the cells to a new flask when recultivated.

2.2.3.3 Transfection of HEK293A cells

Transfection of human HEK293A cells is performed with Lipofectamine 2000® (Thermo Scientific, Schwerte), Opti-MEM transfection medium (Thermo Scientific, Schwerte) and 100ng plasmid DNA (see material). One day prior to transfection, $4*10_4$ cells per well are seeded in 6-well-plates and cultured in DMEM growth medium supplemented with 2% fetal calf serum plus 1% Penicillin/Streptomycin (10,000 U/ml/10,000 µg/ml). Cells are further, as mentioned above for further 24h after transfection. Co-transfection of pEYFP (encodes an enhanced yellow-green variant of the Aequorea victoria green fluorescent protein (GFP)) is performed; thus, preliminary success of transfection may be checked with immunofluorescence microscopy using Zeiss LSM 510 meta microscope and LSM software (Zeiss, Jena).

2.2.3.4 RNA-isolation

For RNA-isolation QIAzol Lysereagents (Qiagen, Hilden) was used. Pelleted cells are washed with PBS (Phosphate-Buffered Saline) before 1 ml of kits lysing reagent, and 250 µl of chloroform (AppliChem, Darmstadt) are added. Separation of the upper aqueous and the lower organic phase is achieved by centrifugation at 14,000 rpm for 15 minutes at 4°C. 500 µl of the upper phase is now transferred to a 1.5 ml tube (Eppendorf, Hamburg). For precipitation of the RNA, 0.8 ml Isopropanol (Sigma-Aldrich, Taufkirchen) is added and followed by another ten minutes of centrifugation. The resulting pellet containing the desired RNA is washed twice with 200 µl of 70% ethanol (AppliChem, Darmstadt) and re-centrifuged again. After removing the supernatant, the RNA pellet is air-dried for 10 minutes and dissolved in RNAse-free water (Gibco, Darmstadt). Quantification and quality control of RNA samples is performed according to chapter 2.2.2.6.

2.2.4 Reporter gene assays (RGA)

For examination of putative regulatory sites on *NLRC4* 5’ UTR, reporter gene assays were used. Reporter gene assays use, i.e. luciferase gene (Pluc2) of Photinus pyralis, which bioluminescence-emission is linear-proportional to gene activity of other examined genes and acts as a surrogate parameter. Luciferase enzyme coded by

Pluc2 is capable of catalysing the oxidation of luciferin to oxyluciferin resulting in the emission of light (Figure 2.3).

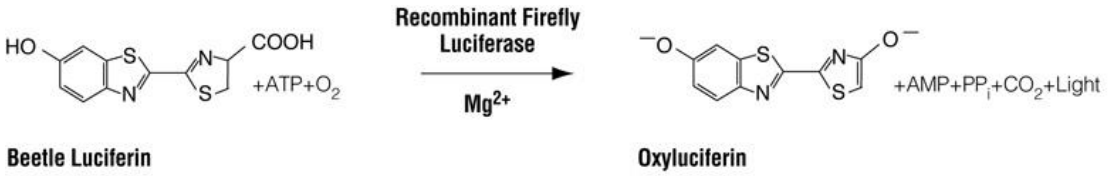

Figure 2.3: Reaction providing bioluminescent signal. Adapted and modified reaction-figure by Promega (Promega, 2015)

Bioluminescent signals were detected by using a luminometer (Tecan infinate m200, Männedorf). For reporter gene constructs containing NLRC4 5' UTR amplicons (see Table Oligonucleotides 2.1.13.4), luciferase reporter vectors pGL4.10[luc2] and pGL4.23[luc2/minP] (Promega, WI, USA) were used. Vectors with pGL4.10 backbone contain no additional promoter, relying on pre-existing promotor region in investigated DNA sequences. In contrast, backbones of pGL4.23 vectors contain a minimal promoter upstream of the luciferase reporter gene. Negative controls were pGL4.10 [luc2] and pGL4.23 [luc2/minP] without NLRC4 5' UTR amplicons in the respective multiple cloning site (MCS), cells only treated with transfection reagent, as well as pGL4.13 [luc2/SV40] acting as a positive control with the SV40-promotor providing a continuous expression of luciferase. Cells used in for reporter gene studies are HEK293A cells, cultivation and transfection were performed in 96-well plates, otherwise according to chapter 2.2.3.3.

2.2.4.1 Cloning of *NLRC4* sequences

Oligonucleotide amplicons used to examine putative regulation sites of the NLRC4 gene (Chromosome 2: 32.488.839 - 32.490.286, 5' UTR, reverse strand) cover different parts of the respective gene and include SNPs rs385076 (position 2: 32.489.859) and rs479333 (position 2: 32.489.159). 14 NLRC4 RGA-constructs with either risk or protective allele configuration were cloned using two luciferase vectors.
Seven NLRC4 RGA-constructs were cloned using two luciferase vectors resulting in 14 RGA-constructs. Amplicons 'both SNPs (IL18+)' and 'both SNPs (0)' (each 1476nt) contain a *NLRC4* 5' UTR sequence with both SNPs in homozygous allele configuration associated to either increased ('IL18+', rs385076 C allele, rs479333 G allele) or normal (protective, rs385076 T allele, rs479333 C allele) IL-18 plasma levels. For localization

of putative regulatory sites, amplicons covering a shorter *NLRC4* 5' UTR and only one of both SNPs with a corresponding allele configuration (rs385076(IL18+) and rs385076(0), 952nt; rs479333(IL18+) and rs479333(0) 716nt; allele configuration as seen above) are used. A short amplicon with *NLRC4* 5' UTR upstream (no SNP/upstream, 318nt) has, according to bioinformatical analyses, a low potential for putative regulatory sites, providing another control for luciferase expression. Primers for amplicon generation were already pre-designed by researchers at the clinic of general and interventional cardiology (UHZ, Hamburg). Details on used primers can be found in table oligonucleotides (2.1.12.3). Template DNA was obtained from human leucocyte samples of the GHS and amplified by utilising PCR. The chosen template DNA sample contains homozygous allele configuration for both SNPs of interest (rs385076 C allele, rs479333 G allele, association to higher IL18 plasma levels, high linkage disequilibrium).

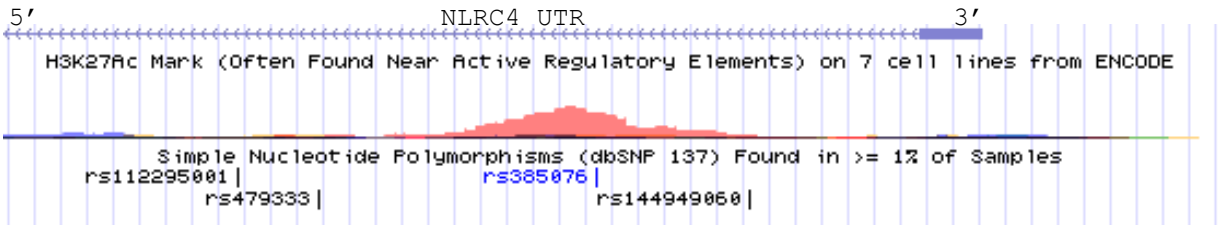

Figure 2.4: Schematic figure of the examined 5' UTR within the NLRC4 gene locus on Chr. 2 (GRCh37 genome data, position nt 32.488.839 - 32.490.286) and location of SNPs. The red area represents the probability to contain regulatory sites. Adapted and modified from UCSC genome browser (Kent et al., 2002).

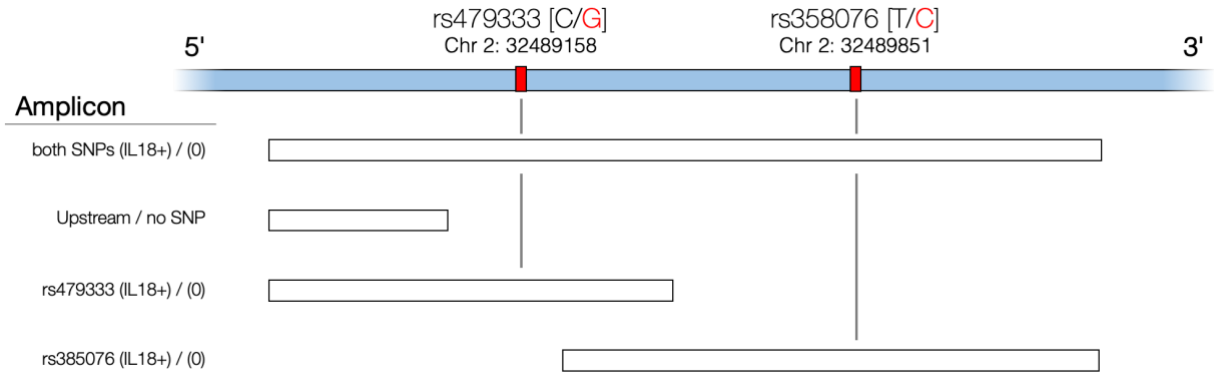

Figure 2.5: Schematic figure of amplicons used in Report Gene Assays. Amplicons contain either one, both or none SNP of interest and are represented proportionally in relation to their original nt-length. Position is displayed according to the covered 5'UTR region.

Table 2.2.17: Details on amplicon-composition used for investigation of *NLCR4* 5' UTR containing SNPs rs385076 and rs479333.

Primer	Amplicon
Forward 1 + Reverse 1	Upstream / no SNP, 318 nt
Forward 2 + Reverse 1	rs479333 (IL18+) and rs479333 (0), 716 nt
Forward 3 + Reverse 1	both SNPs (IL18+) and (0), 1476 nt
Forward 3 + Reverse 2	rs385076 (IL18+) and rs385076 (0) 952 nt

Amplicon generation was done according to the PCR protocol described in chapter 2.2.2.5. Subsequently desired amplicons were isolated through gel-electrophoresis (see 2.2.2.3) and purified by using QIAquick Gel-Extraction Kit (Qiagen, Hilden). Pre-designed primers contain restriction site for the following ligation (forward primers with 'KpnI' restriction site; reverse primers with 'NheI' restriction site, see Table 2.1.12.3). Before cloning *NLCR4* 5'UTR amplicons into luciferase-vectors, ligation into pDRIVE vector is established by using a PCR cloning kit, providing high cloning efficiency and fewer false-positive colonies in comparison to other methods. Purified oligonucleotides are prepared for ligation by enzymatic restriction (see 2.2.2.7) and subsequently ligated into linearized pDRIVE vectors (see 2.2.2.8) for further transformation into competent bacteria strains (see 2.2.5.2) and production stock-plasmid DNA. Sequence analysis is performed for quality control (see 2.2.2.9) before subcloning amplicons into Luciferase-vectors. Thus, restrictive digestion is again performed on sequence controlled pDRIVE vector-amplicons constructs and luciferase reporter gene vectors pGL4.10[luc2] and pGL4.23[luc2/minP] (Promega, WI, USA) with restrictive enzymes KpnI and NheI (New England Biolabs, Frankfurt). Amplicons are purified and ligated into linearized Luciferase-vectors through T4 Ligase. Luciferase-Vector-amplicon constructs are again heat-shock transformed into competent bacterial strains for subsequent plasmid-DNA production and isolation through Mini- and Midi-preparation (see 2.2.4.4). Before Midi-Preparation (production of stock-plasmid DNA), Mini-preparation is done in order to check the success of transfection and plasmid DNA is again controlled by restriction and comparative analysis of resulting fragments and DNA sequencing. Subsequently, desired plasmid DNA is transformed into competent bacterial strains, and Midi-Preparation is done for isolation of stock-plasmid DNA used in further cell-transfection. Following investigations also require luciferase-vector-amplicons plasmids with complementary allele configuration of examined SNPs

(association to normal IL18 plasma levels: rs385076 T allele; rs479333 C allele, homozygous). Several plasmids were altered through of site-directed mutagenesis (see chapter 2.2.2.12). Stocks plasmid DNA of allele altered vectors are amplified analogue to its source plasmids.

2.2.4.2 Transformation of ultra-competent DH5α *E. coli* strain

Ultra-competent DH5α *E. coli* bacteria strain is for used for cloning experiments. Through temperature mediated weakening, the bacteria stay within a condition able to accept foreign plasmid-DNA. The heat-shock method is used with the temperature algorithm containing incubation time on ice for 30 minutes, followed by a heat-shock at 42°C for 1 minute. After cooling on ice for another 5 minutes, the transformation-batches are blended with SOC-medium (see 2.1) approximately 4 times of their respective volume and incubated at 37°C for 45 minutes. After the incubation period, transformation-batches were plated out on Luria-Bertani + ampicillin (LB-amp) agar-plates. Three different volumes of each transformation-batch are used, containing 50 µl, 150 µl, and 300 µl for ideal growth-conditions. Transformation batches are then incubated overnight at 37°C.

2.2.4.3 Cryopreservation of bacteria

For the permanent storage of transformed bacteria, 1 ml bacterial in super optimal broth (SOC)-medium (see 2.1) suspension is treated with glycerol (25% final glycerol concentration) and frozen at -80°C. For re-cultivation, frozen bacterial suspension was scraped off without thawing of the remaining suspension with a sterile inoculation loop and inoculated to LB-ampicillin agar plates.

2.2.4.4 Plasmid-isolation

Plasmid DNA is isolated with mini-preparation and QIAGEN Plasmid Midi Kit from transformed bacterial cultures according to the instructions of the respective kit used.

Mini-preparation

Solitary white colonies (colour coding of pDRIVE vector for successful transformation) are placed into 3 ml of ampicillin-added LB medium. Incubation is done on a shaker at 37°C overnight. 1.5 ml of the resulting suspension is centrifuged for 60 seconds and 13.000 rpm at room temperature. The supernatant is removed, and 100 µl of solution 1 is added and aspirated until pellet is dissolved. Now 200 µl of solution 2 is added to

the suspension and mixed on a shaker, followed by adding 150 µl of solution 3 and incubation on ice for 15 minutes (details on solution 1-3 can be found in 2.1.11). The final suspension is briefly shaken again until a white pellet becomes visible and then centrifuged again for 20 minutes with 13.000 rpm at room temperature.
400 µl of clear supernatant needs to be transferred to a new microtube (Eppendorf, Hamburg) and mixed with 1 ml of ethanol (99%). Another 15 minutes of centrifugation with 13.000 rpm and at room temperature is necessary. The resulting pellet is washed once with 150 µl of ethanol (70%) and re-centrifuged for 2 minutes at the same rpm and temperature. The supernatant may carefully be discarded and the final DNA pellet air-dried of ethanol remnants or 10 minutes. Dissolving has to be done with nuclease-free water.

Midi-preparation

For quantitative higher plasmid-DNA yields, isolation is carried out using Plasmid Plus Midi Kit (Qiagen, Hilden) according to the manufacturer's instructions. Purity and concentration of plasmid-DNA are determined photometrical according to chapter 2.2.2.6 photometric quantification of nucleic acid.

2.2.4.6 Luciferase-Assay measurements

100 µl Bright-Glo Luciferase Assay reagent (Promega) is thawed and added to each well. Multi-well plates (see material) are sealed and frozen for 0.5 hours at -80 °C for cell rupture. Subsequently, cells are thawed at RT and shaken for 5 min at 1400 rpm to ensure entire cell-lysis. After brief centrifugation, 150 µl suspension of each well is transferred to Nunc™ F96 MicroWell™ white Polystyrene plates (Thermo Fisher Scientific, Schwerte). Determination of firefly luciferase bioluminescence is performed using a luminometer (Tecan infinite m200, Männedorf) programmed to detect light emission specific to the luciferase assay.

2.2.5 GHS study cohort

The Gutenberg Health Study is a population-based, prospective, monocentric cohort study conducted since 2007 at the Mainz University Medical Center. Epidemiological data and disease development of cardiovascular, ocular and metabolic disease, as well as disorders of the immune system and psychic disorders, are examined. The first enrolment recruited 15 000 individuals between 35 and 74 years. Variables like lifestyle, psychosocial factors, environment and laboratory parameters and an

additional extensive biomaterial bank for molecular biological investigations are used. The aim is, to gain a more comprehensive understanding and improve risk prediction in individuals regarding each disease entity in a systems biology approach.

2.2.6 Statistical analysis

Data presented in this thesis is displayed in mean and standard deviation (SD). For genotyping, the linkage disequilibrium (LD) and Hardy-Weinberg-Equilibrium (HWE) were calculated with R using package 'genetics' function 'LD' and 'HWE.test'. Clinical characteristics in relation to SNP haplotypes were analysed using R. Analysis of continuous features vs clinical phenotypes was done using one-way ANOVA statistical test, categorically features vs clinical phenotypes was done Chi-squared statistical test. For allele distribution, Pearson's Chi-squared test was applied with a significance threshold of $p > 0.001$. Western blot density values were calculated with mean and standard deviation using R. Densitometric NLRC4 protein values of gel/blot batches were calculated as residuals (random variable within a linear and mixed model) for adjustment of variances between related NLRC4 protein value of each gel/blot batch. Residuals comprise adjustment for gender and age. Reporter gene assay experiments to investigate the putative regulatory region on *NLRC4* 5'UTR are analysed using a one-way ANOVA test with a confidence interval of CI = 95% significance threshold at $p < 0.05$. Analysis and calculations were performed with Graphpad Prism7 (version 7.0a).

3 Results

3.1 Characteristics of GHS study cohort

A cohort of 207 individuals from the GHS study was analysed on the influence of SNP rs385076 risk-allele C and rs479333 risk-allele G on clinical phenotypes. The examined study individuals were selected due to the availability of DNA, PMBC protein lysates and prior performed analysis on caspase-1 activity. The Baseline characteristics are shown in table 3.1.

Table 3.1: Details on characteristics in examined GHS study cohort for the analysis of the association between SNPs rs385076 and rs479333 with clinical parameters.

Study characteristics	GHS study cohort for NLRC4
n	207
Sex = male (%)	103 (50.5)
Age (years mean [SD])	56.32 [10.64]
Prevalence CAD (n [%])	11 [5.5]
History of myocardial infarction (n [%])	9 [4.5]
Diabetes type 1 (%)	14 (6.8)
Systolic bloodpressure (mmHg [SD])	130.56 [17.59]
Diastolic bloodpressure (mmHg [SD])	82.54 [9.66]
CRP (mg/dl mean [SD])	2.42 [2.96]
SNP rs385076	
risk allele (C) frequency (%)	69.95
C/C (n [%])	98 [49.7]
C/T (n [%])	80 [40.6]
T/T (n [%])	19 [9.6]
SNP rs479333	
risk allele (G) frequency (%)	61.33
G/G (n [%])	69 [34.2]
G/C (n [%])	110 [54.5]
C/C (n [%])	23 [11.4]

3.2 Genotyping SNPs rs385076 and rs479333

In order to determine allele configuration, genotyping of rs385076 and rs479333 was performed in DNA samples of 207 GHS subjects. Genotyping of polymorphisms was performed based on q-RT-PCR using TaqMan® SNP genotyping assays (see 2.2.1). Resulting Example of an SNP assay data in Figure 3.1 illustrates the possibility to distinguish between heterozygous and homozygous allele carriers.

VIC

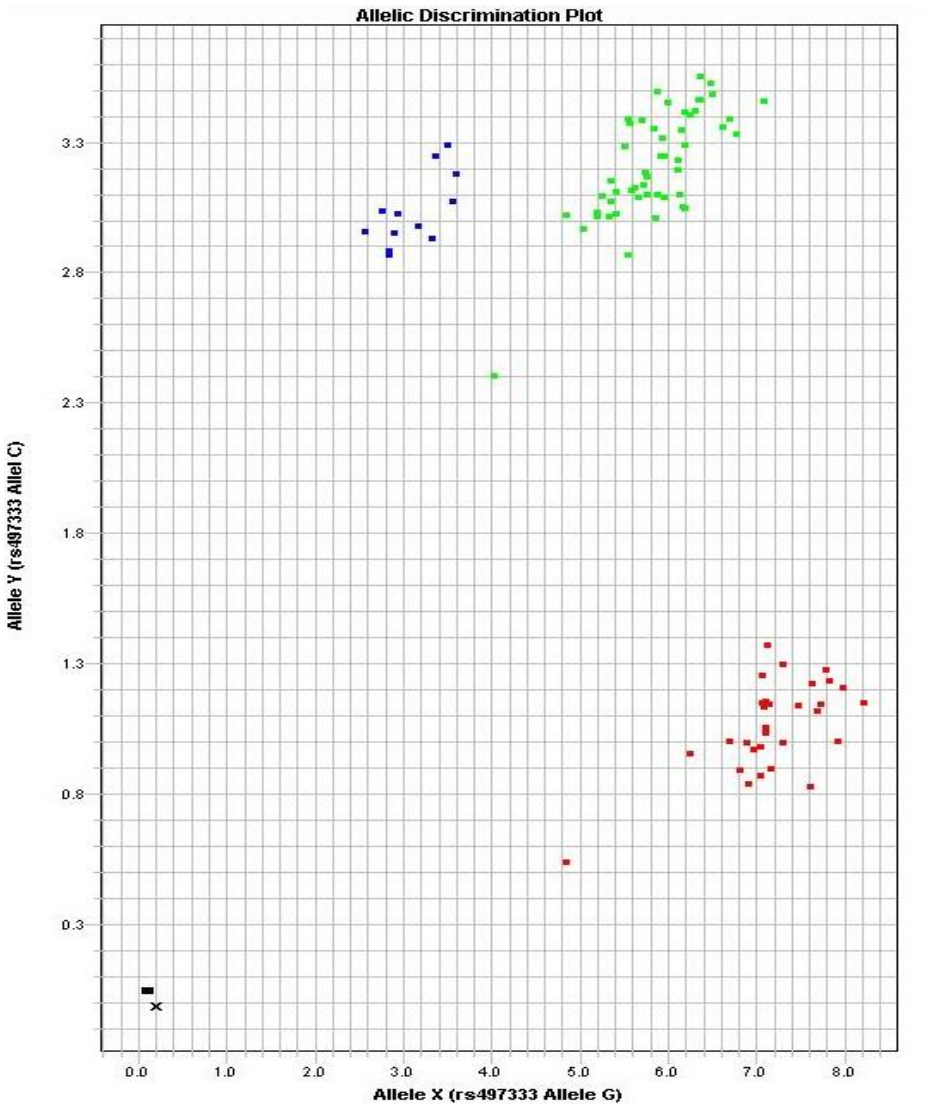

FAM

Figure 3.1: Allelic discrimination plot of TaqMan® rtPCR SNP genotyping assays for SNP rs479333. Alleles of determined SNP (G/C) are shown homozygous or heterozygous represented in either blue, green or red dots (see legend below).

x-axis: signal for allele 1 = guanine (G)	● = homozygous SNP allele G
y-axis: signal for allele 2 = cytosin (C)	● = homozygous SNP allele C
Unit: RFU (relative fluorescence unit)	● = heterozygous SNP allele G/C

Table 3.2: Details on results of genotyping SNP rs385076. Distribution of C and T allele for SNP rs385076 in study cohort by TaqMan® SNP genotyping assays. 11 samples were excluded due to an unclear result in genotyping assays.

SNP	Allele frequency C allele	Allele frequency T allele
rs385076	69.95 %	30.05 %

Table 3.3: Details on results of genotyping SNP rs479333. Distribution of C and G allele for SNP rs479333 in study cohort by TaqMan® SNP genotyping assays. 3 samples were excluded due to an unclear result in genotyping assays.

SNP	Allele frequency G allele	Allele frequency C allele
rs479333	61.33 %	38.67 %

Based on the bioinformatical analysis on data of 196 individuals out of the examined 207 individuals from GHS, SNP rs385076 and rs479333 represent the linkage disequilibrium of D' = 0.823 when both SNPs present haplotypes with risk alleles. Therefore, the analysis confirmed SNP rs479333 to be a proxy SNP to SNP rs385076. Respective significance value for allele distribution was $p = 0.7362$ for rs385076 and $p = 0.0396$ and rs479333 at a significance threshold of $p > 0.001$ within Hardy-Weinberg-Equation.

3.3 NLRC4 protein-expression in PBMC samples

In order to quantify NLRC4 protein expression, quantitative Western blot analysis was performed in PBMC protein lysates of 207 GHS individuals (see 2.2.2.2) and further correlated with respective haplotypes. Densitometric analysis was used for determination of NLRC4/CARD12 antibody labelled protein-bands (see figure 3.2). Adjustment of normalized NLRC4 protein density values was performed to gender, age and batches of PBMC samples. No significant association between the lead-SNP rs385076 SNPs risk allele C and NLRC4 protein levels in healthy individuals could be observed ($p = 0.081$). Nevertheless, when evaluating the effect of the proxy SNP rs479333 (LD = 0.823), a borderline association of the IL-18-lowering C allele and decreasing NLRC4 protein levels was observed ($p = 0.049$).

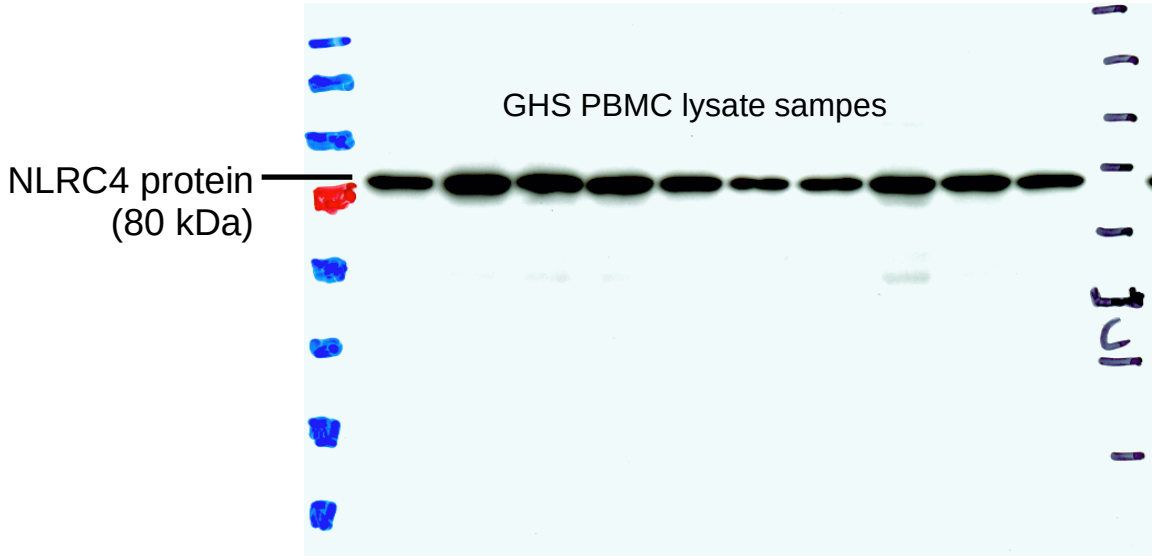

Figure 3.2: Example of Western-Blot transfer showing proteins NLRC4 (80 kDa) staining after incomplete washing process in GHS PBMC lysate samples. PageRuler™ Prestained Protein Ladder (10 to 180 kDa) was used (left side, red mark ~ 70 kDa).

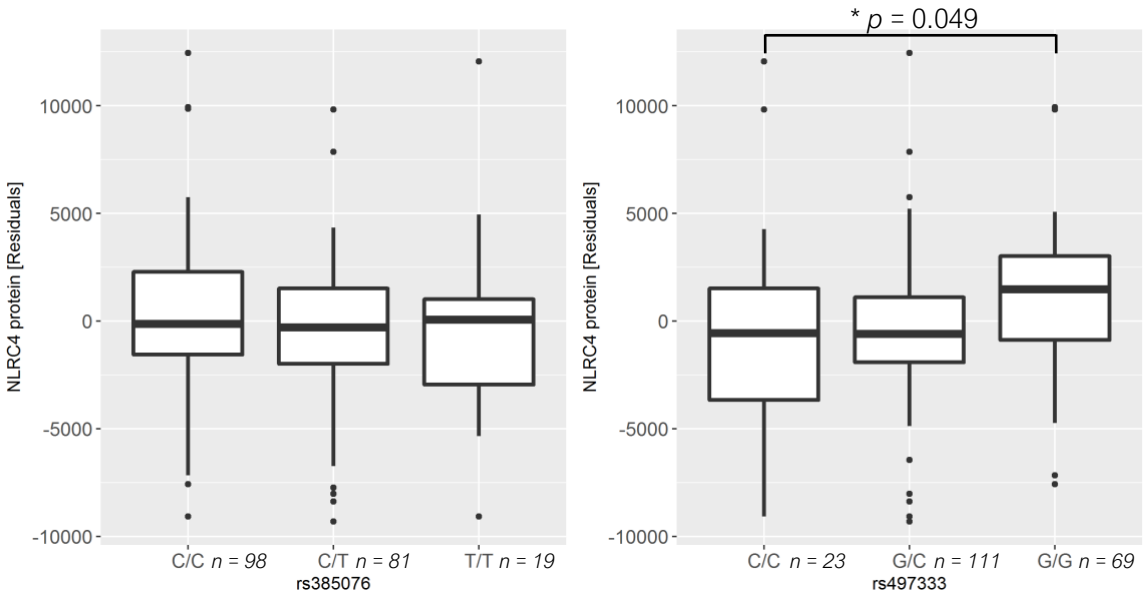

Figure 3.3 a + b: Correlation of SNP rs385076 (3.3a) and rs479333 (3.3b) haplotype to NLRC4 Protein expression in PBMC lysates of 207 GHS individuals. Genotyping has been performed before the determination of protein-levels with TaqMan® SNP genotyping assays (see 3.1). Densitometric protein values are shown as residuals and have been normalized, adjusted to sex and age, as well as invariances between gel/blot charge (batches, 10-12 individuals per batch). SNP rs479333 protective allele C showing borderline significance (p = 0.049) for decreased NLRC4 protein levels. SNP rs385076 risk allele C showed no significant association to increased NLRC4 protein levels (p = 0.081).

3.4 Analysis of putative regulatory effects of SNPs rs385076 and rs479333 within NLRC4 5'UTR by Reporter Gene Assay

Since investigations on protein-level provided a borderline association between *NLRC4* protein-expression and SNP rs479333 allele frequency, putative regulatory sites within the NLRC4 5' UTR in proximity to SNPs rs385076 and rs479333 may alter transcriptional activity. Further investigations were performed using a luciferase reporter gene assay (RGA) system (Promega, WI, USA) in a cell culture-based system. Putative regulatory sites within the 5' UTR of the *NLRC4* aligning SNPs rs385076 and rs479333 would result in increased expression of luciferase, thus increased emission of bioluminescence. Vectors used for RGA studies contained NLRC4 5'UTR, as illustrated in figure 2.5. The longest DNA fragments contained SNPs rs385076 and rs479333 in homozygous allele configuration associated to either increased ('IL18+', rs385076 C allele, rs479333 G allele) or normal (protective, rs385076 T allele, rs479333 C allele) IL-18 plasma levels. For comparison, vectors with shorter NLRC4 5' UTR contain either only one SNP in corresponding allele configuration (rs385076(IL18+) and rs385076(0); rs479333(IL18+) and rs479333(0)), or only upstream 5' UTR without respective SNPs (Upstream / no SNP). By comparing the emitted bioluminescence, the *NLRC4* 5' UTR is tried to be 'mapped' for putative regulatory sites. According to bioinformatical analyses, *NLRC4* 5' UTR in vectors containing 'Upstream / no SNP' amplicons show low potential for putative regulatory sites and therefore are used as an additional control for determination of baseline luciferase expression. Positive and negative controls used within luciferase assays are listed in chapter 2.2.4. After transfection of *NLRC4* RGA-constructs, as well as vectors for positive and negative control in HEK 293A cells, the readout of cell-culture plates was performed in a luminometer (see 2.2.4.6). Additional confirmation of transfection efficiency was established by simultaneous transfection of pEYFP and means of fluorescence microscopy (see figure 3.4 a-d).

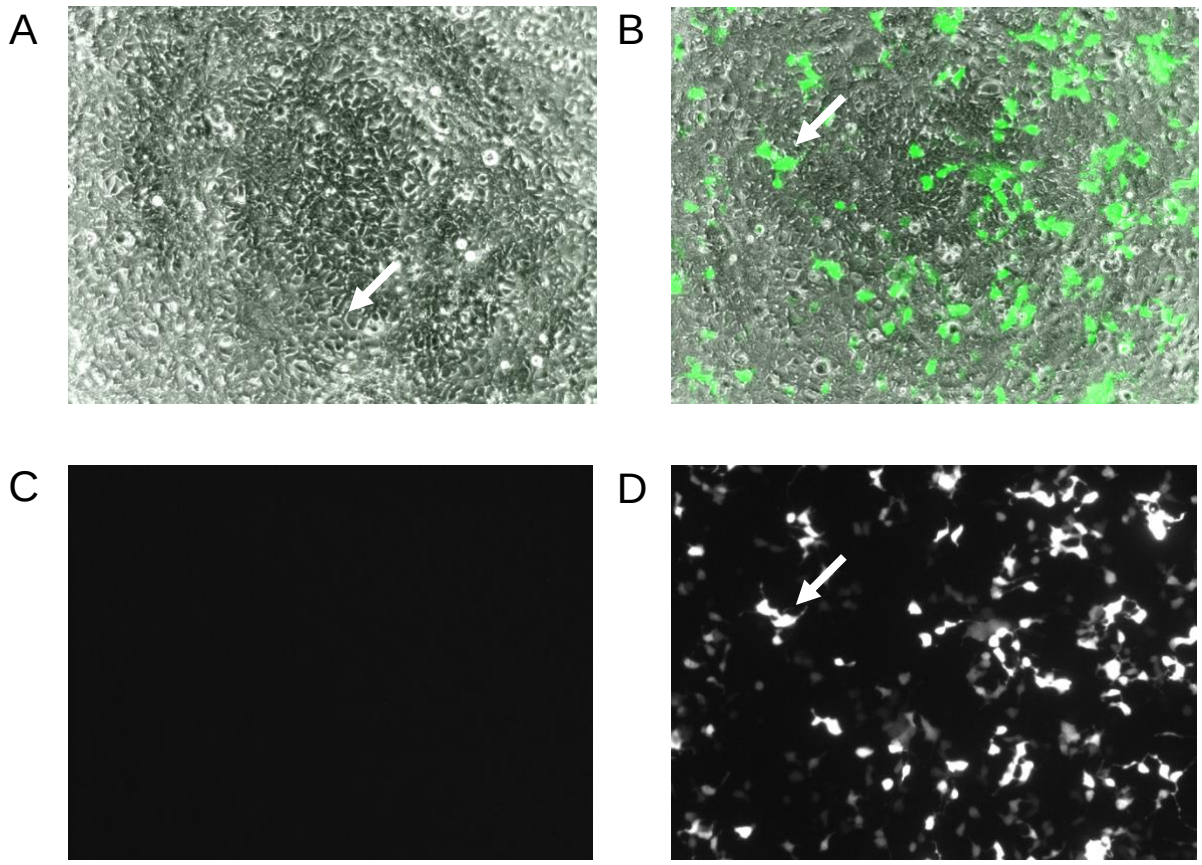

Figure 3.4 a-d: Fluorescence microscopy of HEK 293A after transfection with GFP using lipofectamine 2000 transfection reagent. Images on the left (A + C) showing untreated cells, images on the right (B + D) showing cells treated with lipofectamine 2000 + pYEFP, approximate transfection efficiency was estimated at around 20% - 30%. White arrows are indicating solitary cells.

Figures 3.5 a-c show statistical analysis of luciferase reporter gene assay experiments with *NLRC4* RGA-constructs using pGL4.10[luc2] and pGL4.23[luc2/minP] vectors. Controls for analysis were *NLRC4* RGA-construct (Upstream / no SNP) which represent the emission of *NLRC4* 5' UTR without SNPs and suggested regulatory sites, RGA vectors with continuously high bioluminescence emission (pGL4.13), as well as empty pGL4.10[luc2] and pGL4.23[luc2/minP] vectors and HEK293A cells without RGA vectors. In pGL4.10[luc2] luciferase vectors a significant increased bioluminescence emission was observed, when comparing RGA constructs 'Upstream / no SNP' with 'both SNPs (IL18+)' [*$p = 0.028$] and 'rs385076(normal)' [*$p = 0.004$]. Also, significantly increased emissions were observed when comparing NLRC4 RGA-constructs 'both(IL18+)' vs. 'both(normal)' [* $p = 0.048$] and '479333(IL18+)' vs.

‘479333(normal)’ [*p = *0.044*], in both cases in favour for the latter. In pGL4.23[luc2/minP] RGA-constructs only those containing a ‘rs385076(IL18+)’ amplicon showed a significantly increased bioluminescence emission in comparison to ‘Upstream / no SNP’ RGA-constructs [*p = *0.044*]. The pGL4.13 vector with continuously high emission of bioluminescence showed a mean bioluminescence-value of 1.791.614 RLU. The empty pGL4.10[luc2] and pGL4.23[luc2/minP] vectors were measured with 4967 RLU and respectively 7128 RLU of bioluminescence.

Data provided by reporter gene assay investigations might indicate an influence of SNPs rs385076 and rs479333 allele frequency on *NLRC4* gene-regulation. In total, RLU values shown are approximate to RLU of empty-vector controls; thus, experimental data has to be evaluated critically (see 4.2).

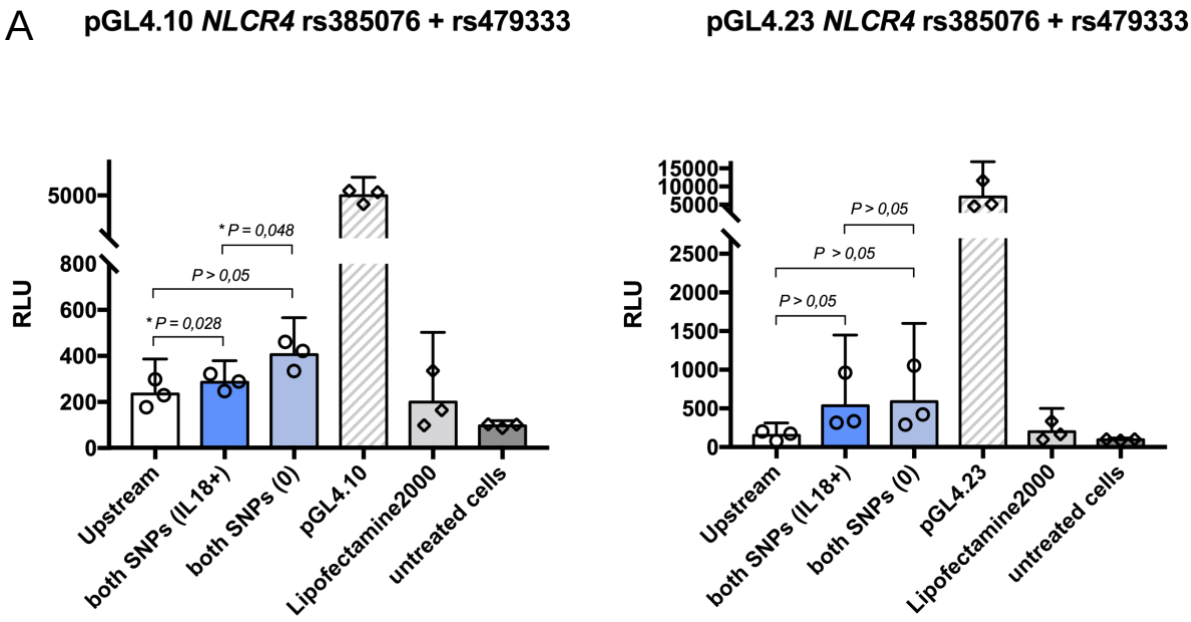

Figures 3.5 A: Statistical analysis of luciferase reporter gene assays for investigations on putative regulatory sites within NLRC4 exon 2, 5’ UTR. Data from three independent experiments (n = 3, mean of each three technical replicates) was analysed using one-way ANOVA statistical test with multiple comparisons. Significance level for every calculation was p = 0.05, error-bars within graphs represent confidence-interval (CI = 95%). Figure 3.5 A shows results for the vectors containing amplicons with both SNPs rs385076 and rs479333, figure 3.5 B and C the results of respective vectors with either SNP rs385076 or rs479333. Addition figures see below.

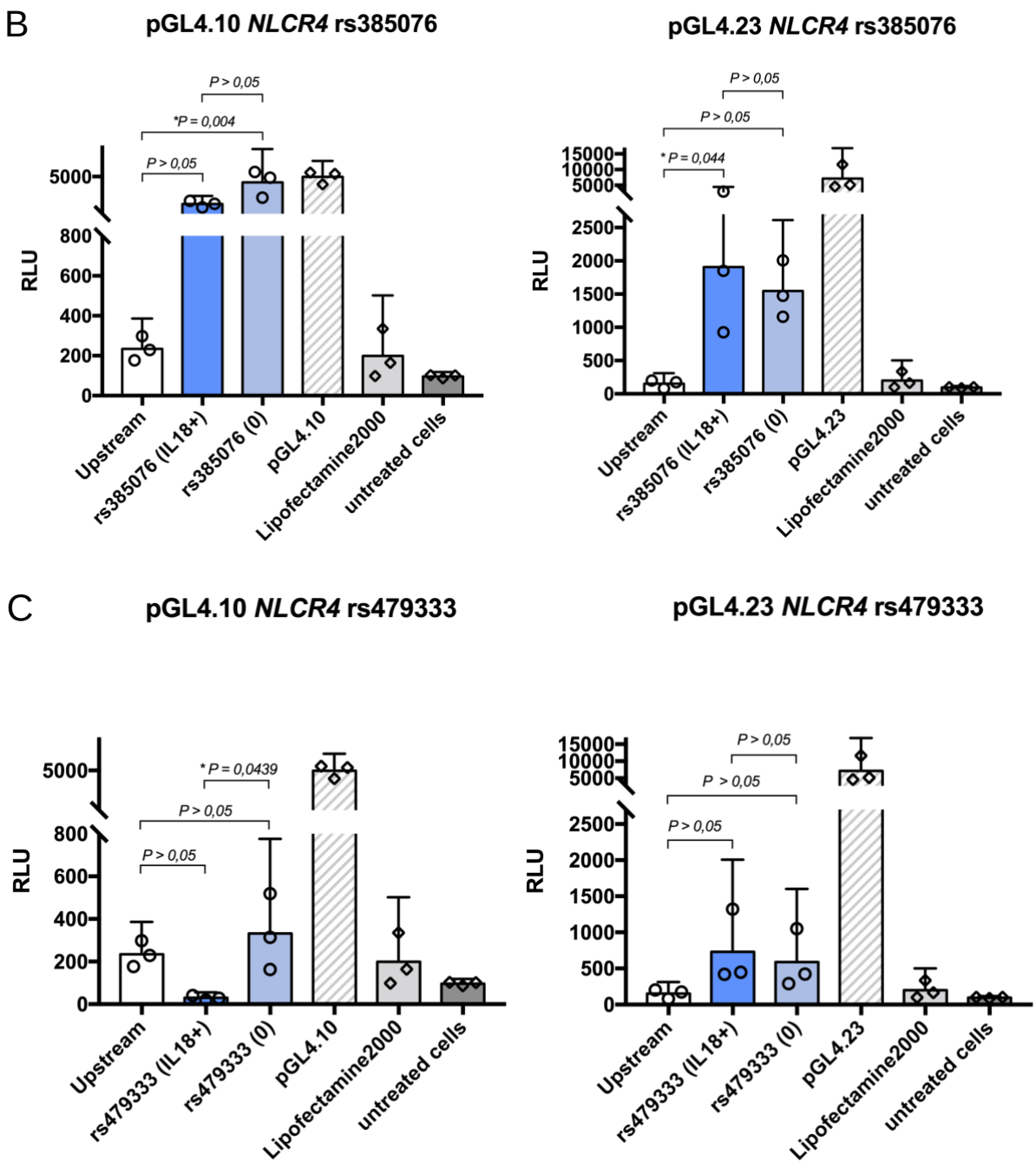

Figures 3.5 B and C: Description see below figure 3.5 A.

3.5 *NLRC4* expression profile in untreated and LPS stimulated HEK293A

As described above, the evaluation of SNPs rs385076 and rs479333 relation to NLRC4 protein-expression provided data on an association of rs479333 protective C allele. Additionally, putative regulatory sites within *NLRC4* 5' UTR could not be revealed using reporter gene assays. For identification of previously unknown genetic loci in proximity, qPCR experiments in HEK293A cell-model were designed. Up-/down-regulation of putative genes associated with *NLRC4* may be facilitated and analysed by siRNA-induced *NLRC4* knockdown. Literature provided data on *NLCR4* expression in HEK293A cell as well as induction through LPS (Martinon et al., 2002); thus preliminary qPCR experiments aimed to establish baseline expression of *NLCR4* in untreated HEK293A cells were carried out according to chapter 2.2.6. Untreated HEK293A cells did not show sufficient expression of *NLCR4* for further knockdown experiments. Further investigations on NLRC4 expression in HEK293A cells within this study have not been continued.

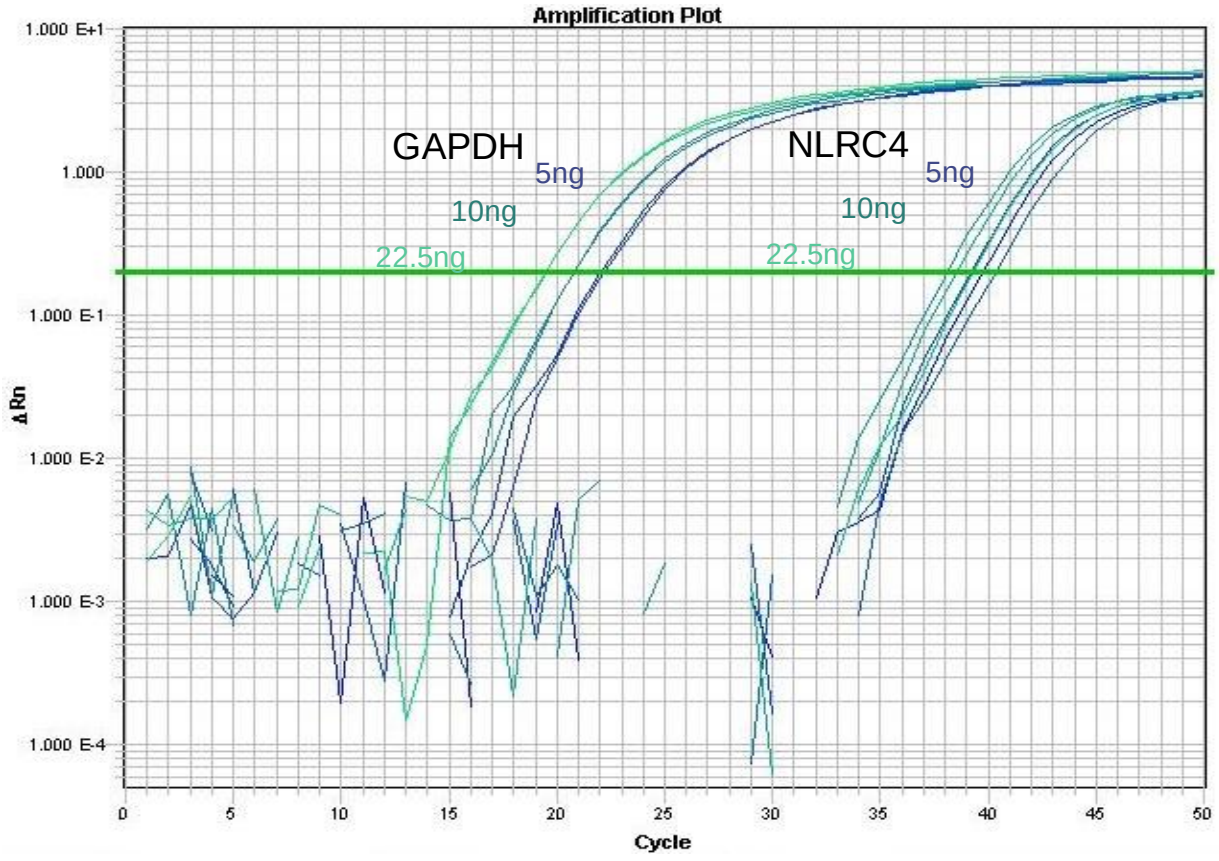

Figure 3.6: NLRC4 and GAPDH gene expression in untreated HEK293A rtPCR experiments. Three different cDNA concentrations have been used, Ct threshold was manually set to 0.2.

Table 3.4: Median Ct-values of NLRC4 gene expression in HEK293A rtPCR experiments. Untreated HEK293 have been used for preliminary experiments.

Gene	cDNA Concentration [ng]	median Ct-value
NLRC4	5	39.7333
NLRC4	10	39.7529
NLRC4	25	38.5557
GAPDH	5	22.1095
GAPDH	10	20.7871
GAPDH	25	19.4342

3.6 Association of SNP rs385076 and rs479333 on NLRC4 protein levels and clinical parameters

Literature data showed an association of IL-18 plasma levels and coronary artery disease, cardiovascular mortality (Blankenberg et al., 2003, Jefferis et al., 2011) and an effect on increased atherosclerotic plaque instability (Mallat et al., 2001). In relation to chapter 1.2.5, the influence of genetic polymorphisms on the association of IL-18 plasma levels and cardiovascular mortality was analysed by a GWAS meta-analysis within an international cohort (total n = 9,562 of Gutenberg Health Study (GHS I), Framingham Heart Study (FHS) and Kooperativen Gesundheitsforschung in der Region Augsburg F4 (KORA F4)). Additionally, replication of results was performed in three additional cohorts (n = 3.348 of Atherogene, Monitoring in Trends and Determinants in Cardiovascular Diseases (MONICA), KORA S1/2/3 and Prospective Epidemiological Study of Myocardial Infarction (PRIME)-Study). The analysis confirmed SNP rs385076 on chromosome 2 ($p_{meta} < 2.4*10^{-45}$), as well as SNP rs11606049 on chromosome 11 ($p_{meta} < 4.6*10^{-35}$) to be the most significant at a genome-wide significance threshold of $p_{meta} < 5*10^{-8}$ (see figure 1.5) (Zeller et al., 2015).

In addition to the wet-lab data, the association of clinical parameters and SNP rs385076, as well as its proxy SNP rs479333 haplotypes, were statistically analysed. The selection of evaluated clinical parameters is summarized in table 3.1. The overall median age of GHS individuals within the study cohort was 56.3 years (SD = 10.64), and the gender-distribution showed 50.5 % men. IL-18 plasma levels were measured in samples of the majority of GHS study-individuals and showed an overall mean of 217.39 [pg/mL] (CI = 168.22, 283.85). No IL-18 plasma levels were measured in the study cohort analysed within this thesis.

More detailed analysis showed, that only for SNP 385076 haplotypes there was a significant difference between risk allele (C) and protective allele T, when comparing CRP plasma levels (* p = 0.005, mean comparison with one-way ANOVA statistical test; haplotypes C/C = 3.16 [SD = 3.47 mg/dl] vs. C/T = 1.85 mg/dl [SD 1.87 mg/dl] vs. T/T = 1.48 mg/dl [SD = 1.64 mg/dl]). There was no significant difference, when comparing prevalence of CAD, history of MI, incidence of Diabetes type 1, blood pressure

Table 3.5: Association of SNP rs385076 haplotypes with clinical characteristics within GHS study cohort of this thesis, mean-comparison was conducted with one-way ANOVA statistical test.

SNP rs385076	C/C	C/T	T/T	p-Value
n	98	80	19	
Sex = Male (n [%])	53 [54.1]	38 [48.1]	5 [26.3]	0.084
Age (mean [SD])	56.91 [10.35]	55.67 [10.49]	57.37 [11.39]	0.691
Prevalence CAD (n [%])	6 [6.2]	3 [3.9]	2 [11.1]	0.486
History of MI (n [%])	7 [7.2]	2 [2.6]	0 [0.0]	0.215
Diabetes type 1 (%)	5 [5.1]	6 [7.6]	2 [10.5]	0.621
SBP (mmHg [SD])	130.37 [18.70]	131.27 [16.21]	129.47 [19.23]	0.923
DBP (mmHg [SD])	81.59 [10.19]	84.32 [9.10]	80.05 [8.03]	0.086
CRP (mg/dl mean [SD])	3.16 [3.47]	1.85 [1.87]	1.48 [1.64]	* *0.005*
NLRC4 residual (mean [SD])	15509.83 [4382.31]	14173.06 [4643.29]	14825.00 [5493.76]	0.275

Table 3.6: Association of SNP rs479333 haplotypes with clinical characteristics within GHS study cohort of this thesis, mean-comparison was conducted with one-way ANOVA statistical test.

SNP rs479333	C/C	C/T	T/T	p-Value
n	23	110	69	
Sex = Male (n [%])	8 [34.8]	56 [51.4]	36 [52.2]	0.311
Age (mean [SD])	56.17 [11.34]	55.58 [10.84]	57.80 [10.07]	0.398
Prevalence CAD (n [%])	3 [13.6]	4 [3.8]	4 [5.9]	0.186
History of MI (n [%])	2 [9.1]	4 [3.7]	3 [4.4]	0.542
Diabetes type 1 (%)	0 [0.0]	9 [8.3]	5 [7.2]	0.366
SBP (mmHg [SD])	123.96 [15.83]	130.69 [16.56]	133.07 [19.43]	0.099
DBP (mmHg [SD])	80.70 [8.11]	83.63 [8.61]	81.71 [11.48]	0.258

CRP (mg/dl mean [SD])	2.52 [3.55]	2.36 [3.09]	2.58 [2.61]	0.884
NLRC4 residual - (mean [SD])	14253.19 [6017.77]	14457.99 [4312.70]	16060.02 [4416.87]	0.136

Statistical analysis within the superordinated GHS study cohort showed a significant association of IL-18 plasma levels and prevalence of atherosclerotic plaque and history of MI, but not the prevalence of CAD, when adjusted for SNPs rs385076 and rs479333 risk allele dosage (see table 3.7). A meta-analysis of the superordinate group of study individuals (GHS, KORA F4, AtheroGene, PRIME, and MONICA/KORA S1/S2/S3) were able to show a protective effect of rs385076 non-risk allele T on cardiovascular mortality with an age and gender-adjusted hazard ratio = 0.78 (CI = 95%, 0.62 – 0.98; **p* = 0.03) (Zeller et al., 2015).

Table 3.7: Correlation of IL-18 plasma levels on clinical parameters within individuals superordinated GHS study cohort, adjusted for sex and gender, as well as rs385076 and rs479333 risk allele dosage.

			adjusted for rs385076 (C) and rs479333 (G) allele	
	ß-value (CI)	**p-value**	**ß-value (CI)**	**p-value**
Prevalence plaque	0.043 (0.016, 0.069)	0.0017 *	0.038 (0.004, 0.072)	0.028 *
Prevalence CAD	0.003 (-0.051, 0.057)	0.9136	0.026 (-0.033, 0.084)	0.39
History of MI	0.056 (-0.009, 0.121)	0.0892	0.114 (0.043, 0.185)	0.0016 *

4 Discussion

The study aimed to assess the influence of *NLRC4* genetic variants SNP rs385076 (C/T) and rs479333 (G/C) on *NLRC4* protein expression in PBMC lysates of both, healthy individuals and those with CAD. Also, the identification of putative regulatory sites within *NLRC4* 5'UTR in proximity to SNPs rs385076 and rs479333 was tried to be performed utilising a luciferase reporter gene assay system. In an approach to further investigate the functional relation between respective SNPs and *NLRC4* expression, an *NLCR4* qPCR model in HEK293A cells was tried to be established. This thesis showed that:

1) Genetic variant rs385076 haplotypes did not show an association to *NLRC4* protein expression, whereas proxy SNP rs479333 showed an association with borderline significance.
2) Within the *NLRC4* 5'UTR, no putative regulatory sites could be identified using Luciferase reporter gene assays. The examined *NLRC4* 5'UTR either contained SNP rs385076 or proxy SNP rs479333, both SNPs or upstream 5' UTR without examined SNPs.
3) Within the examined study cohort, SNP rs385076 protective allele T shows to be associated with significantly lower mean CRP plasma levels in comparison to risk allele C.

In the following, results are discussed in the context of current literature and study-limitations.

4.1 Regulation of NLRC4-inflammasome and influence of genetic variants rs385076 and rs479333 on NLRC4 protein-levels

Correlating NLRC4 protein-levels with SNP allele configurations, SNP rs479333 risk allele G showed an association to increased NLRC4 protein-expression with borderline-significance (p = 0.049), whereas SNP rs385076 did not show an allele-specific correlation (p = 0.81). Nevertheless, biostatistical meta-analysis highlighted a putatively functional association between SNP rs385076 and IL-18 concentrations (see chapter 1.3, figure 1.4). About those findings, the relevance of the total NLRC4 protein amount in relation to IL-18 maturation should be critically evaluated.

Since SNP rs385076 is located within *NLRC4* untranslated region, a direct influence on IL-18 concentration is unlikely. According to current literature, mechanisms how the

NLRC4-inflammasome regulates pro-IL-18 processing may instead depend on a variety of cofactors and ligands (i.e. NAIPs), regulation of transcriptional and translational activity, as well as posttranslational modification (Latz et al., 2013, Monie, 2017). I.e. protein phosphorylation is an essential regulatory mechanism in various cell processes. A recent study demonstrated the necessity of posttranslational phosphorylation of NLRC4 protein Ser533 after NLRC4-Inflammasome assembly for further caspase-1 activation and induction of pyroptosis. PKCδ has been postulated as candidate kinase responsible for NLRC4 Ser533 phosphorylation (Qu et al., 2012).
In comparison to the NLRC4-Inflammasome, other NLR-inflammasomes such as NLRP3- and NLRP1-Inflammasomes need the adaptor molecule apoptosis-associated speck-like protein containing CARD (ASC or PYCARD) for caspase-1 recruitment (Franchi et al., 2009). A similar posttranslational modification was shown for ASC, where phosphorylation of Tyr144 within its CARD is crucial for caspase 1 recruitment. Syk and JNK were identified as kinases responsible for respective phosphorylation (Hara et al., 2013). Regulation of phosphorylating kinases involved in innate and adapted immunity is yet not fully understood and may also be influenced by functional genetic variants.
Diverse regulatory processes in cells depend on feedback mechanisms. The amount of NLRC4 protein and the bioactivity of stimulated NLRC4-inflammasomes, i.e. cytokine secretion, may also regulate further *NLRC4* expression in an inflammation limiting manner. In LPS-stimulated and siRNA mediated *NLRC4* knockdown experiments in macrophages, significantly higher IL-18 concentrations could be found when *NLRC4* knockdown led to decreased NLRC4 protein-expression presumably mediated by ERK, JNK or p38 mitogen-activated protein kinase (MAPK) pathways (Zhu et al., 2016). Those findings support the idea of feedback mechanisms and highlight, that total NLRC4 protein-amount may have to be seen independently from IL-18 cytokine secretion and subsequent cardiovascular mortality.

Consideration should also be paid to technical limitations, possibly influence measured results. Monocytes are known to express NLRC4 protein sufficiently; hence, prior studies on *NLRC4* gene expression in relation to SNP rs385076 and rs479333 haplotype and their particular effect on IL-18 were performed in this cell-type.
In this thesis, the quantification of NLRC4 protein was performed in PBMC samples of GHS individuals, which could constitute a different *NLRC4* mRNA and protein

expression profile. PBMCs are any mononuclear cells, comprising T- and B-lymphocytes, natural killer cells additionally to monocytes. Recent studies indicate them to be suitable for analysis of *NLRC4* mRNA expression (Harris et al., 2018). Also, the small sample size of approximately 200 individuals may not be suitable for valid assumptions. Besides, the individuals from population-based GHS are both healthy and CAD affected individuals. When using western blot and gel electrophoresis for protein quantification, densitometric quantification may be highly subjective. Densitometric quantification has to be done by one individual to minimize technical errors. The western blot method is affiliated to the antibody-dependent methods, which comprise, i.e. enzyme-linked immunosorbent assays (ELISA) or protein immunoprecipitation (IP). The ELISA method measures the emission of light after a respective enzyme is specifically linked through protein-antigen-antigen-enzyme interaction (Engvall and Perlmann, 1972). The IP method is addressing a specific antigen of the target protein with a concordantly specific antibody bound to a solid medium (magnetic or agarose beats) which may be further analysed through matrix-assisted laser desorption/ionization (MALDI) spectrometry (Kaufmann, 1995). Both methods avoid invariances through subjective analysis. A spectrometric approach for protein quantification without prior labelling of proteins by antibodies is possible as well (Liebler and Zimmerman, 2013). When analysing individuals of both groups without further differentiation, samples of healthy individuals with a risk-associated genotype may have NLRC4 mRNA protein amounts with not congruently increased IL-18 plasma levels. Protein-lysates from study-individuals may also be compromised through storage circumstances, thus potentially suffocated protein-degradation. Additionally, only one technical replication was used when performing western blot analysis due to low stock volumes of cell-lysates, restricting comparability of samples down to actin-normalisation and statistical calculation of residuals (see chapter 2.8).

Analysis of NLRC4 provided data on four differently expressed isoforms. When expressed, only isoform 2 and 4 include 5'UTR exon 2, which comprises the examined genetic variants. As far as understanding, the antibody used within western blot analysis does not distinguish between different isoforms; thus, actual NLRC4 protein amount may be different from what was measured by densitometry. Differentiation between NLRC4 protein isoforms may contribute to more specific conclusions (see chapter 4.2).

4.2 Putative regulatory influence of SNP rs385076 comprising *NLRC4* 5’ UTR on gene expression

Our understanding of regulatory mechanisms as mentioned in chapter 4.1 elaborates, i.e. intramolecular interactions like ligand interaction, conformational changes with subsequent gain- or loss of functions, the influence of co-factors, but also regulatory effects on a transcriptional level. Recent research increasingly focuses on how, e.g. genetic variants can orchestrate transcriptional regulation. Researchers within the study-group associated with this thesis continued investigations on SNP rs385076 and were able to identify a novel transcriptional factor binding site in the *NLRC4* locus surrounding SNP rs385076. If underlying SNP genotype presents risk-allele C, it is enabling the surrounding genetic area to gain functionality as a transcription factor binding site for PU.1. In vitro experiments showed significantly increases *NLRC4* expression in luciferase RGA, when incubating cells with PU.1. However, RGA experiments performed within this study used amplicons, which do not cover the probable and later confirmed transcriptional factor binding side. Due to technical limitations, RGA-constructs with long amplicons may provide false-negative results in RGA studies. Since proxy SNP rs479333 also was shown to provide a significant association to increased IL-18 plasma levels and cardiovascular mortality and additionally is located further upstream of lead SNP rs385076, obviously within study design the sequence downstream of SNP rs385076 was neglected. Using PU.1 in this studies RGA experiments might not have led to the observed impact on NLRC4 gene expression. Additionally, NLRC4 isoform 2 and 4 comprise of the NLRC4 5’ UTR exon 2, whereas NLRC4 isoform 3 does not include the 5’ UTR exon 2, but covers a more extended sequence downstream of rs385076. When examining the NLRC4 5’UTR, not only the presence of transcriptional factor PU.1 and rs385076 allele configuration may be necessary for increased transcriptional activity, but also a specific isoform of NLRC4.

It is known, that within the Interleukin-1 subfamily transcriptional gene regulation of IL-1ß is also mediated by PU.1. A respective transcriptional factor binding site is located within the IL-1ß gene core promoter region (Kominato et al., 1995). As a response to inflammation-inducing signals like LPS or interleukins themselves, PU.1 synergistically acts with transcriptional factor CCAAT/enhancer-binding-protein (C/EBP-ß) when interacting with myeloid differentiation primary response gene 88 (MyD88). Subsequently, *IL-1ß* expression is upregulated through the C/EBP-ß pathway (Bent et

al., 2018). So far, a direct linkage between upregulated *IL-18* or *NLRC4* and the C/EBP-ß pathway is not known. However, the inflammatory response of macrophages, i.e. interleukin-secretion is, as far as known, regulated by signalling pathways like ERK1/2, p38 and JNK-MAPK (Song et al., 2015, Wang et al., 2015). Involvement of PU.1 leading to altered *NLRC4* expression may result through associated signalling pathways like C/EBP-ß and MAPKs. Since their relation to posttranslational phosphorylation of NLRC4 is described, an influence of the particular NLRC4-inflammasome activity could be postulated.
Additionally, differential expression of *NLRC4* isoforms in dependence to SNP rs385076 allele configuration was found. If SNP rs385076 presents non-risk allele T, significantly more isoform 1 or 3 without NLRC4 5' UTR is expressed (Zeller et al., 2015). Recent research has been highlighting various transcriptome subcategories of endogenous noncoding RNA (enRNA) like long noncoding RNA (lncRNA), microRNA (miRNA) and circular RNA (circRNA) (Beermann et al., 2016). The function of circRNA was linked to atherosclerosis through mechanisms like miRNA binding or induction of alternative transcription (Fan et al., 2017). Since differential transcription of *NLRC4* 5'UTR was shown to be in dependence to haplotypes of rs385076 and rs479333 correlating with higher IL-18 plasma levels hence atherosclerosis, more complex regulatory pathways, appear to be possible. Further research is still necessary to understand those regulatory processes indicating functionality of genetic variants.

Technical circumstances have to be considered, limiting the interpretation of the RGA experiments performed within this study. When measuring RLU in reporter gene assays, empty pGL4.10 [luc2] and pGL4.23 [luc2/minP] vectors expressed higher relative luminescence values than pGL4.10 [luc2] and pGL4.23 [luc2/minP] Vector containing *NLRC4* 5'UTR (see chapter 3.3). A possible explanation could be the influence of transcription inhibiting regions. Considering that not only promotor regions but also genetic repressors for transcription act synergistically together and, in common, are located in proximity, also repressing genetic elements could have been ligated into the luciferase vectors with the selected *NLRC4* sequences. Therefore, inhibitory influence on transcriptional activity is possible. Another limitation may be that vector stocks could have been damaged due to the cloning process. Also, single steps within the cloning process could have been unsuccessful, leading to serial mistakes. Controversially to this explanation, constructs have been checked through sequencing

after final steps of the cloning process in the manner of quality control, unintentional mutations within the inserted *NLRC4* region were corrected by side-directed mutagenesis but furthermore not sequenced again. Regarding the manufactures advice, cell-lines used within reporter gene assay experiments should present an expression profile suitable for the investigated genetic locus. Even though previous experiments for NLRC4 were performed in immunological cell lines, HEK293A was used within this study's experiments. Lately, HEK293A cells were demonstrated to be suitable for RGA experiments on *NLRC4,* as mentioned above.

4.3 *NLRC4* gene expression analysis in HEK293A cells – approach to establish a siRNA mediated knockdown

Complementary to prior *NLRC4* protein expression and *NLRC4* reporter gene assay experiments, siRNA induced *NLRC4* mRNA knockdown model in HEK293A was tried to be established. As mentioned above, the relation of rs385076 and rs479333 to genetic up- and downstream regions in the vicinity to the investigated *NLRC4* 5'UTR (2:32.488.839 – 2:32.490.286; GRCh37 genome dataset) was discussed. Recent research shows NLRC4 to have a change of function when co-expressed with SUG 1, leading to caspase 8 dependent apoptosis instead of caspase 1 related pyroptosis (Kumar et al., 2010). Other recent investigations demonstrated the relevance of CARD- and Pyrin-only proteins (COP, POP), having structural similarity to CARD and Pyrin, which provide them with dimerization-limiting abilities (Kersse et al., 2007, Le and Harton, 2013). With this functional relation and their genetic locus being in proximity to the caspase 1 locus on Chr. 11, the expression of, i.e. SUG1 or COP/POP might be influenced through *NLCR4* mRNA knockdown. Based on current data of the STRING Consortium 2018 database (Szklarczyk et al., 2017), genes summarized in table 4.1 appear to be co-expressed with *NLRC4* without a so far known functional relation. However, all of the named genes can be considered to be functional within the innate immune system.

First approaches of *NLRC4* mRNA knockdown were performed in HEK293A cell-line. Measurement of untreated HEK293A cells showed insufficiently high ct-values for NLRC4 at different concentrations for used cDNA (median ct-value for all cDNA concentration = 39.3473). An explanation could be due to the used HEK293A cell-line. HEK293A might not be suitable for experiments on *NLRC4* gene-expression since not belonging to an immune-system associated cell-line. Since other studies used

HEK293A for similar experiments on *NLRC4* gene-expression, shown results are most likely due to a technical error. GAPDH ct-values (median ct-value for all cDNA concentration = 20.7769) suggested a sufficient amount of template cDNA. However, further experiments should avoid technical and study design errors: cDNA concentrations have not been re-measured after rtPCR rewriting of mRNA into cDNA, therefore having a high probability for technical mistakes. An adequate stimulus like LPS might be necessary for adequate induction of *NLRC*4 gene-expression. Also, the used kit or a single reagent could have been compromised.

Table 4.1: Genes co-expressed with *NLRC4* according to recent STRING Consortium 2018 database (STRING V10.5).

	Gene	ENSEMBLE ID	STRING score*
LILRB2	Leukocyte immunoglobulin-like receptor, subfamily B (with TM and ITIM domains), member 2	ENSP00000375629	0.461
IGSF6	Immunoglobulin superfamily, member 6	ENSP00000268389	0.457
C1orf162	Chromosome 1 open reading frame 162	ENSP00000344218	0.435
CD163	CD163 molecule	ENSP00000352071	0.426

* The STRING score is an approximate probability that a predicted link exists between two enzymes/proteins in the same metabolic map in the KEGG database (low confidence - 0.15 (or better), medium confidence - 0.4, high confidence - 0.7, highest confidence - 0.9).

4.4 Relation between SNPs rs385076 and rs479333 haplotypes to clinical characteristics

Statistical analysis of clinical parameters relevant for CAD (see table 3.1) and haplotypes of examined SNPs showed significantly lower CRP plasma levels when SNP rs385076 protective allele T is present (see chapter 3.6, table 3.6). Other clinical characteristics showed no significant correlation, and there was no significant association with SNP rs479333 haplotypes. As elaborated in chapter one, inflammation is increasingly understood as a cornerstone within the pathogenesis of cardiovascular disease (Aday and Ridker, 2019). The observed association underlines the influence of yet not fully understood genetics like rs385076 on the overall

inflammation. Still, the association of SNP rs385076 haplotype may also merely be a confounder, since experimental studies are necessary to examine and validate the actual molecular pathway. Also, since blood samples of the study cohort have not been measured for IL18 plasma levels, no additional adjustment to IL-18 plasma levels was able to be included within the analysis.

4.5 Limitations

General limitations of this study have to be considered. The GHS Individuals are of European descent. The relations of genetic variants to clinical phenotypes may present controversially in other ethnicities. Additionally, blood IL-18 levels corresponding to the samples used within this thesis were not measured. Hence, the correlation of SNP rs385076 and rs479333 haplotypes, corresponding NLRC4 protein amount and clinical parameters of the study cohort could not be adjusted to IL-18 plasma levels within the analysis. Examined genetic variants are not exonic polymorphisms causing known functional changes in amino acid sequences, but untranslated polymorphisms. Reporter gene assay experiments were able to show a transcriptional factor binding side for PU.1 if risk associated haplotype of rs385976 is present. Findings on the association of SNP rs479333 and NLRC4 protein amount, as well as PU.1 binding site, negate a spurious relationship of the variants within the *NLRC4* locus to increased cardiovascular risk.

4.6 Outlook

The association of *NLRC4* variants and NLRC4 protein expression remains unclear. Further experiments may address technical difficulties as elaborated in chapter 4.1 and consider other methods of quantification. Following studies may use already known variables like *NLRC4* isoform and phosphorylation status for study-design and analysis. A functional relation between *NLRC4* variants and IL-18 plasma levels could be concluded if IL-18 plasma levels of analysed individuals are known. With the differential expression of *NLRC4* isoforms demonstrated, reporter gene assays have to be evaluated if being suitable for further investigation on regulatory mechanisms of the *NLRC4* SNP rs385076 locus. Still, the circumstance of differential expression highlights the importance of ncRNA and should be addressed in further experiments. Additionally, other SNPs within the *NLRC4* locus presenting a similar significant association with IL-18 plasma levels may be examined for potential regulatory

mechanisms. Also, since higher CRP plasma levels showed an association the SNP risk allele C, studies like the CANTOS trial highlighting the relevance of inflammation in atherosclerosis, other pro-inflammatory mediators might be evaluated in clinical and experimental studies whether being associated to known genetic variants relevant for CAD.

Therapeutical approaches in primary and secondary prevention of CAD address multiple aspects of disease development. A significant target in therapy focuses on the cholesterol hypothesis, thus decreasing LDL-, and increasing HDL-levels in order to lower the risk for atherosclerosis (Shapiro and Fazio, 2016). Further individualization of therapy is an emerging research topic in cardiovascular medicine, addressing inflammation and increasingly individual genetic background. The significance of targeting inflammation to reduce the risk for CAD is proven by several major studies like the Pravastatin or Atorvastatin Evaluation and Infection Therapy (PROVE-IT) and the Improved Reduction of Outcomes: Vytorin Efficacy International (IMPROVE-IT) trial. When considering both studies, they outlined the relevance of residual inflammatory risk (hsCRP ≥ 2mg/L under treatment with cholesterol-lowering agents) within 43% - 47% of 18.924 individuals leading to the reoccurrence of ACS (Ridker, 2017). Moreover, the concept of inflammation in atherosclerosis and its possibilities as therapeutical target was recently redefined, when the Canakinumab Anti-inflammatory Thrombosis Outcomes Study (CANTOS) reported a significantly decreased risk for cardiovascular events in 10.061 post-MI patients with residual inflammatory risk under the treatment of Canakinumab (monoclonal interleukin 1-ß inhibitor) (Ridker et al., 2017).

This study aimed to gain insight into how the genetic variants rs385076 and rs479333 within the 5’ UTR of *NLRC4* may regulate the secretion of pro-inflammatory IL-18. IL-18 emerged to play a significant role in CAD-development and risk-prediction (Mallat et al., 2001, Blankenberg et al., 2003). As far as known, the induction of caspase 1 is limited to NLRC4, NLRP-1, -5, -6, -7,-12 and ASC (Broderick et al., 2015, Winkler and Rosen-Wolff, 2015). With regards to NLRC4, known interacting proteins are interferon-gamma-inducible protein 16 SUG-1 and PKCδ (Kumar et al., 2010, Qu et al., 2012, Latz et al., 2013, Winkler and Rosen-Wolff, 2015, Monie, 2017). Experimental data on validation of the hypothesis of genetic variants rs385076 and rs473999 influence the NLRC4 protein expression and subsequently IL-18 concentrations did provide a borderline significant relation between SNP rs479333 risk allele G with increased

NLRC4 protein amounts. Other relations could not be validated in multiple experimental approaches. As discussed in chapter 4.2, binding of PU.1 leads to differential expression of *NLRC4*. Further studies may investigate regulatory effects of lncRNA or circRNA from noncoding *NLRC4* RNA including SNP rs385076 an rs479333. The mechanisms on how different ncRNA regulate cell-processes, in general, are still to be fully understood and require further studies.

About the general and technical limitations explained above, samples from either healthy or CAD individuals could be preselected in future experiments, leading to better comparison and rule out the bias explained in chapter 4.1. Also, cells used in upcoming cell-culture based experiments on *NLRC4* 5'UTR and associated genetic variants could be exchanged with THP-1 cells-lines. THP-1 are monocyte precursor cells of the immune system, potentially more suitable for experimental work on inflammatory processes in atherosclerosis by their reaction to corresponding stimuli like smoke, PAMPs or DAMPs. Literature shows THP-1 to sufficiently express *NLRC4* for reporter gene assays and investigations on the effect of MicroRNA on gene expression have already be established (Jami, 2017).

Since CAD is to be understood as a multifactorial disease, comprehensive research on how heredities regulate pathogenesis and other associated pathways is still needed and may identify novel drug targets aiming for individualised medicine.

5 Summary | Zusammenfassung

5.1 Summary

Prior large-scaled, population-based studies identified the association of specific polymorphisms (SNPs) and increased IL-18 plasma levels, indicating a genetic locus with a potentially functional association (*NLRC4* gene, lead SNP rs385076, $p_{meta} = 2.4 * 10^{-45}$). It was suggested, that the SNPs may influence the NLRC4 protein expression and subsequent activation of pro-inflammatory NLRC4-inflammasome, leading to increased maturation of IL-18. The pro-inflammatory IL-18 was functionally linked to CAD development as well as utilized as a risk-predictive biomarker (Mallat et al., 2001, Blankenberg et al., 2003). This thesis examined the relation between genetic variants SNP rs385076 (C/T; 2:32.264.782) and rs479333 (G/C; 2:32.264.089) within the 5'UTR of the *NLRC4* locus (2:32.223.625 to 32.266.682, p22.3) and NLRC4 protein expression as well as clinical characteristics within a selected study-cohort of the GHS. Also, novel regulatory sites within the respective 5'UTR were tried to be identified.

NLRC4 protein expression was measured by western blot analysis in PBMC lysates of both, healthy individuals and those with CAD. The identification of putative regulatory sites within *NLRC4* 5'UTR in proximity to SNPs rs385076 and rs479333 was tried to be performed utilizing a luciferase reporter gene assays in a HEK293A cell model. In an approach to further investigate the functional relation between respective SNPs and NLRC4 expression, an NLCR4 qPCR model in HEK293A cells was tried to be established. Within the examined study cohort, SNP rs385076 protective allele T was associated with significantly lower mean CRP plasma levels in comparison to its risk allele C.

In conclusion, SNP rs385076 haplotypes did not show an association with *NLRC4* protein expression, whereas SNP rs479333 showed an association with borderline significance ($p = 0.049$). Within the *NLRC4* 5'UTR, no putative regulatory sites could be identified using luciferase reporter gene assays. Still, the following investigators were able to identify a novel transcriptional factor binding site for transcriptional factor PU.1, if rs385076 risk-allele C is present. When incubating cells with PU.1, a significantly increases luciferase activity, as well as increased *NLRC4* expression of *NLRC4* isoforms, were observed in luciferase reporter gene assays and qPCR experiments.

The findings highlight the importance of the *NLRC4* gene locus on immunological aspects of CAD development and subsequently, cardiovascular mortality. Further experimental studies may address novel regulatory pathways, i.e. the influence of non-coding RNA.

5.2 Zusammenfassung

Vorangegangene, populationsbasierte Studien identifizierten die Assoziation von spezifischen genetischen Polymorphismen (SNPs) innerhalb des NLRC4 Locus auf Chr. 2 und erhöhten IL-18-Plasmaspiegeln (NLRC4-Gen, Lead-SNP rs385076, $p_{meta} = 2,4 * 10^{-45}$). Ein funktioneller Zusammenhang war naheliegend, in dem die SNPs die NLRC4-Proteinexpression beeinflussen. Eine Mehr-Aktivierung des pro-inflammatorischen NLRC4-Inflammasoms könnte zu einer erhöhten Prozessierung und Sekretion von IL-18 führen. Das pro-inflammatorische Zytokin IL-18 konnte bereits in vorangegangenen experimentellen und klinischen Studien funktionell mit vermehrter Arteriosklerose der Koronargefäße assoziiert, sowie als risikoprädiktiver Biomarker identifiziert werden (Mallat et al., 2001, Blankenberg et al., 2003). Diese Arbeit untersuchte den Zusammenhang zwischen den genetischen Polymorphismen SNP rs385076 (C/T; 2:32.264.782) und SNP rs479333 (G/C; 2: 32.264.089) innerhalb der 5'UTR des *NLRC4* Locus (2:32.223.625 - 32.266.682, p22.3), und der NLRC4-Proteinexpression sowie klinischer Charakteristika innerhalb einer ausgewählten Studienkohorte. Ebenfalls wurde versucht, innerhalb der den SNPs naheliegende Abschnitten der *NLRC4* 5'UTR potentielle regulatorische Areale zu identifizieren.

Die NLRC4-Proteinexpression wurde in PBMC-Lysaten von sowohl gesunden sowie kardiovaskulär erkrankten Individuen mittels Western-Blot gemessen. Innerhalb eines HEK293A Zellkultur Modells wurde durch Luciferase Reportergen Assays die definierte *NLRC4* 5'UTR auf potentielle regulatorische Einheiten untersucht. Um die funktionelle Beziehung der SNPs mit der *NLRC4* Expression detaillierter zu analysieren, wurde ein *NLRC4*-qPCR Modell in HEK293A-Zellen für Knockdown- und Überexpressions-Experimente innerhalb eines ersten Ansatzes versucht zu etablieren. In einer statistischen Aufarbeitung der untersuchten GHS Studienkohorte konnte das protektive SNP rs385076 Allel T mit signifikant niedrigeren mittleren CRP-Plasmaspiegeln assoziiert werden.

Es konnte gezeigt werden, dass SNP rs479333 Haplotypen eine grenzwertig signifikante Assoziation zu einer erhöhten NLRC4 Proteinexpression zeigen (*p =

0.049, SNP rs479333 Risiko allele G). Ein ähnlicher Zusammenhang wurde für SNP 385076 nicht gefunden. In Reportergen Assay Versuchen innerhalb dieser Studie konnte keine regulatorische Einheit auf der untersuchten *NLRC4* 5'UTR identifiziert werden. In folgenden Experimenten der Studiengruppe ließ sich jedoch im gleichen Versuchsmodell unter Zugabe des Transkriptionsfaktor PU.1 eine neue Transkriptionsfaktorbindungsstelle auf der um SNP 385076 auf der *NLRC4* 5'UTR identifizieren, sofern bei diesem das Risiko Allel C vorlag. Es zeigte sich hierbei eine signifikant erhöhte Aktivität der Luciferase sowie *NLRC4* Expression verschiedener *NLRC4* Isoformen in Luciferase Reportergen Assays bzw. qPCR Experimenten.

Die Bedeutung des *NLRC4* Locus innerhalb der immunologischen Pathogenese von Arteriosklerose, und damit der kardiovaskulären Mortalität konnte in dieser Studie weiterführend gezeigt werden. Auch wenn die genauen molekularen Mechanismen weiterhin unklar sind, weisen die Ergebnisse auf die Relevanz von beispielsweise nichtkodierender RNA in der Regulation des Immunsystems hin.

6 Index of abbreviations

ACS	Acute coronary syndrome
ASC (PYCARD)	Apoptosis-associated speck-like protein containing CARD
C/EBP-ß	CCAAT/enhancer-binding protein beta
CAD	Coronary Artery Disease
CAPS	Cryopyrin-associated periodic syndromes
CARD	Caspase recruitment domain
cDNA	Complementary DNA
Chr.	Chromosome
COP	CARD-only Protein
Ct value	Threshold cycle
DAMP	Damage-associated Molecular Patter
DNA	Deoxyribonucleic acid
ERK	Extracellular-signal Regulated Kinase
ELISA	Enzyme-linked immunosorbent assays
GWAS	Genome wide association studies
GM-CSF	Granulocyte-macrophage colony-stimulating factor
HDL	High density lipoprotein
HEK293A	Human embryonic kidney cells 293
IFN-γ	Interferon-gamma
IFI16	Interferon-gamma-inducible protein 16
IGIF	Interferon-gamma inducing factor
IL-1β	Interleukin 1β
IL-18	Interleukin 18
IL-18 BP	Interleukin 18 binding protein
IL-18 R1	Interleukin 18 receptor 1
IL-6	Interleukin 6
IL-4	Interleukin 4
IL-10	Interleukin 10
IL-13	Interleukin 13
IL-2	Interleukin 2
IL-8	Interleukin 8

JNK	c-Jun N-terminal kinase
LD	Linkage disequilibrium
LDL	Low-density lipoprotein
LDL-R	Low Density Lipoprotein-Receptor
LPS	Lipopolysaccharide
LRR	Leucin-Rich-Repeat Domain
lncRNA	Long non-coding RNA
MALDI	Matrix-assisted laser desorption/ionization Spectrometry
MAPK	Mitogen-activated protein kinase
MAS	Macrophage activation syndrome
MCR	Macrophages scavenger receptors
MCS	Multiple cloning site
MI	Myocardial infarction
mRNA	Messenger RNA
MyD88	Myeloid differentiation primary response gene 88
NAIP	NLR-family, Apoptosis Inhibitory Protein
NBD/NACHT	Nucleotide Binding Domain
NHEJ	Non-homologous end joining
NLRC4	NOD-Like receptor protein CARD 4
NLRP1	NACHT, LRR and PYD domains-containing protein 1
NLRP12	NACHT, LRR and PYD domains-containing protein 12
NLRP3	NACHT, LRR and PYD domains-containing protein 3
NLRP5	NOD-like receptor family pyrin domain containing 5
NLRP6	NOD-like receptor family pyrin domain containing 6
NLRP7	NACHT, LRR and PYD domains-containing protein 7
NOD	Nucleotide-binding oligomerization domain
NTC	Non-Template Control
oxLDL	Oxidative Low-density lipoprotein
p38	P38 mitogen-activated protein kinases
PAMP	Pathogen-associated Molecular Pattern
PBMC	Peripheral Blood Mononuclear Cell
PBS	Phosphate-Buffered Saline
PCR	Polymerase Chain reaction
POP	Pyrin-only Protein

PYD	Pyrin Domain
q-RT-PCR	Quantitative real time Polymerase chain reaction
QTL	Quantitative trait loci
RNA	Ribonucleic acid
RT	Room temperature
siRNA	Small interfering RNA
SMC	Smooth muscle cell
SNP	Single nucleotide polymorphism
SUG-1 (PSMC5)	Suppressor of gal 1 (proteasome 26S subunit, ATPase 5)
Syk	Spleen tyrosine kinase
TGF-ß	Tumour-Growth-Factor-ß
TGF-ß1	Tumour-Growth-Factor-ß1
TLR	Toll like receptors
TNF	Tumour-Necrosis-Factor
TNF-α	Tumour-Necrosis-Factor-alpha
VCAM-1	Vascular cell adhesion protein 1
VLDL	Very low-density lipoprotein
ZFN	Zinc-finger nuclease

7 Index of tables and figures

7.1 Tables

7.2 Figures

8 References

ADAY, A. W. & RIDKER, P. M. 2019. Targeting Residual Inflammatory Risk: A Shifting Paradigm for Atherosclerotic Disease. *Front Cardiovasc Med,* 6**,** 16.

AHOLA-OLLI, A. V., WURTZ, P., HAVULINNA, A. S., AALTO, K., PITKANEN, N., LEHTIMAKI, T., KAHONEN, M., LYYTIKAINEN, L. P., RAITOHARJU, E., SEPPALA, I., SARIN, A. P., RIPATTI, S., PALOTIE, A., PEROLA, M., VIIKARI, J. S., JALKANEN, S., MAKSIMOW, M., SALOMAA, V., SALMI, M., KETTUNEN, J. & RAITAKARI, O. T. 2017. Genome-wide Association Study Identifies 27 Loci Influencing Concentrations of Circulating Cytokines and Growth Factors. *Am J Hum Genet,* 100**,** 40-50.

APPLIEDBIOSYSTEMS. 2019a. *TaqMan Gene Expression Assay solutions* [Online]. Available: https://tools.thermofisher.com/content/sfs/brochures/taqman-gex-brochure.pdf [Accessed 20. june 2019].

APPLIEDBIOSYSTEMS. 2019b. *TaqMan® SNP Genotyping Assays* [Online]. Available: https://assets.thermofisher.com/TFS-Assets/LSG/manuals/MAN0009593_TaqManSNP_UG.pdf [Accessed 20. june 2019].

BEERMANN, J., PICCOLI, M. T., VIERECK, J. & THUM, T. 2016. Non-coding RNAs in Development and Disease: Background, Mechanisms, and Therapeutic Approaches. *Physiol Rev,* 96**,** 1297-325.

BENT, R., MOLL, L., GRABBE, S. & BROS, M. 2018. Interleukin-1 Beta-A Friend or Foe in Malignancies? *Int J Mol Sci,* 19.

BERGSBAKEN, T., FINK, S. L. & COOKSON, B. T. 2009. Pyroptosis: host cell death and inflammation. *Nat Rev Microbiol,* 7**,** 99-109.

BJORKBACKA, H. 2015. Atherosclerosis: cell biology and lipoproteins. *Curr Opin Lipidol,* 26**,** 67-9.

BLANKENBERG, S., LUC, G., DUCIMETIERE, P., ARVEILER, D., FERRIERES, J., AMOUYEL, P., EVANS, A., CAMBIEN, F., TIRET, L. & GROUP, P. S. 2003. Interleukin-18 and the risk of coronary heart disease in European men: the Prospective Epidemiological Study of Myocardial Infarction (PRIME). *Circulation,* 108**,** 2453-9.

BLANKENBERG, S., TIRET, L., BICKEL, C., PEETZ, D., CAMBIEN, F., MEYER, J., RUPPRECHT, H. J. & ATHEROGENE, I. 2002. Interleukin-18 is a strong predictor of cardiovascular death in stable and unstable angina. *Circulation,* 106**,** 24-30.

BRODERICK, L., DE NARDO, D., FRANKLIN, B. S., HOFFMAN, H. M. & LATZ, E. 2015. The inflammasomes and autoinflammatory syndromes. *Annu Rev Pathol,* 10**,** 395-424.

BROZ, P. 2015. Inflammasome assembly: The wheels are turning. *Cell Res,* 25**,** 1277-8.

BRUCE BLAUS, B. C. S. 2014. Medical gallery of Blausen Medical 2014. *WikiJournal of Medicine.*

CHEN, M. C., CHEN, C. J., YANG, C. H., WU, C. J., FANG, C. Y., HSIEH, Y. K. & CHANG, H. W. 2007. Interleukin-18: a strong predictor of the extent of coronary artery disease in patients with unstable angina. *Heart Vessels,* 22**,** 371-5.

CONSORTIUM, C., SAMANI, N. J., DELOUKAS, P., ERDMANN, J., HENGSTENBERG, C., KUULASMAA, K., MCGINNIS, R., SCHUNKERT, H., SORANZO, N., THOMPSON, J., TIRET, L. & ZIEGLER, A. 2009. Large scale association analysis of novel genetic loci for coronary artery disease. *Arterioscler Thromb Vasc Biol,* 29**,** 774-80.

CONSORTIUM, C. A. D., DELOUKAS, P., KANONI, S., WILLENBORG, C., FARRALL, M., ASSIMES, T. L., THOMPSON, J. R., INGELSSON, E., SALEHEEN, D., ERDMANN, J., GOLDSTEIN, B. A., STIRRUPS, K., KONIG, I. R., CAZIER, J. B.,

JOHANSSON, A., HALL, A. S., LEE, J. Y., WILLER, C. J., CHAMBERS, J. C., ESKO, T., FOLKERSEN, L., GOEL, A., GRUNDBERG, E., HAVULINNA, A. S., HO, W. K., HOPEWELL, J. C., ERIKSSON, N., KLEBER, M. E., KRISTIANSSON, K., LUNDMARK, P., LYYTIKAINEN, L. P., RAFELT, S., SHUNGIN, D., STRAWBRIDGE, R. J., THORLEIFSSON, G., TIKKANEN, E., VAN ZUYDAM, N., VOIGHT, B. F., WAITE, L. L., ZHANG, W., ZIEGLER, A., ABSHER, D., ALTSHULER, D., BALMFORTH, A. J., BARROSO, I., BRAUND, P. S., BURGDORF, C., CLAUDI-BOEHM, S., COX, D., DIMITRIOU, M., DO, R., CONSORTIUM, D., CONSORTIUM, C., DONEY, A. S., EL MOKHTARI, N., ERIKSSON, P., FISCHER, K., FONTANILLAS, P., FRANCO-CERECEDA, A., GIGANTE, B., GROOP, L., GUSTAFSSON, S., HAGER, J., HALLMANS, G., HAN, B. G., HUNT, S. E., KANG, H. M., ILLIG, T., KESSLER, T., KNOWLES, J. W., KOLOVOU, G., KUUSISTO, J., LANGENBERG, C., LANGFORD, C., LEANDER, K., LOKKI, M. L., LUNDMARK, A., MCCARTHY, M. I., MEISINGER, C., MELANDER, O., MIHAILOV, E., MAOUCHE, S., MORRIS, A. D., MULLER-NURASYID, M., MU, T. C., NIKUS, K., PEDEN, J. F., RAYNER, N. W., RASHEED, A., ROSINGER, S., RUBIN, D., RUMPF, M. P., SCHAFER, A., SIVANANTHAN, M., SONG, C., STEWART, A. F., TAN, S. T., THORGEIRSSON, G., VAN DER SCHOOT, C. E., WAGNER, P. J., et al. 2013. Large-scale association analysis identifies new risk loci for coronary artery disease. *Nat Genet,* 45**,** 25-33.

DE CATERINA, R., D'UGO, E. & LIBBY, P. 2016. Inflammation and thrombosis - testing the hypothesis with anti-inflammatory drug trials. *Thromb Haemost,* 116**,** 1012-1021.

DINARELLO, C. A. 2018. Overview of the IL-1 family in innate inflammation and acquired immunity. *Immunol Rev,* 281**,** 8-27.

DINARELLO, C. A. & FANTUZZI, G. 2003. Interleukin-18 and host defense against infection. *J Infect Dis,* 187 Suppl 2**,** S370-84.

ELEFTHERIADIS, M. S. 2011. *Genetic variability of IL-18 and risk of cardiovascular disease.* Inauguraldissertation Doktorgrad Medizin, Johannes Gutenberg-Universität.

ENGVALL, E. & PERLMANN, P. 1972. Enzyme-linked immunosorbent assay, Elisa. 3. Quantitation of specific antibodies by enzyme-labeled anti-immunoglobulin in antigen-coated tubes. *J Immunol,* 109**,** 129-35.

ERDMANN, J., KESSLER, T., MUNOZ VENEGAS, L. & SCHUNKERT, H. 2018. A decade of genome-wide association studies for coronary artery disease: The challenges ahead. *Cardiovasc Res*.

FAN, X., WENG, X., ZHAO, Y., CHEN, W., GAN, T. & XU, D. 2017. Circular RNAs in Cardiovascular Disease: An Overview. *Biomed Res Int,* 2017**,** 5135781.

FRANCHI, L., EIGENBROD, T., MUÑOZ-PLANILLO, R. & NUÑEZ, G. 2009. The inflammasome: a caspase-1-activation platform that regulates immune responses and disease pathogenesis. *Nature immunology,* 10**,** 241-247.

HANSSON, G. K. 2005. Inflammation, atherosclerosis, and coronary artery disease. *N Engl J Med,* 352**,** 1685-95.

HANSSON, G. K. & LIBBY, P. 2006. The immune response in atherosclerosis: a double-edged sword. *Nat Rev Immunol,* 6**,** 508-19.

HARA, H., TSUCHIYA, K., KAWAMURA, I., FANG, R., HERNANDEZ-CUELLAR, E., SHEN, Y., MIZUGUCHI, J., SCHWEIGHOFFER, E., TYBULEWICZ, V. & MITSUYAMA, M. 2013. Phosphorylation of the adaptor ASC acts as a molecular switch that controls the formation of speck-like aggregates and inflammasome activity. *Nat Immunol,* 14**,** 1247-55.

HARRIS, L., COLEMAN, L., KHOO, K., BIZZINTINO, J., FRANKS, K. M., PRASTANTI, F., OO, S., MCCRAE, C., OBERG, L. & BORLAND, M. L. 2018. NLRC4 Gene Variants Are Associated with mRNA Expression Levels in Children Having an Asthma

Exacerbation. *D54. INTERPLAY OF DIVERSE CELLULAR AND MOLECULAR PATHWAYS IN ASTHMA AND AIRWAY DISEASE.* American Thoracic Society.

HE, M., CORNELIS, M. C., KRAFT, P., VAN DAM, R. M., SUN, Q., LAURIE, C. C., MIREL, D. B., CHASMAN, D. I., RIDKER, P. M., HUNTER, D. J., HU, F. B. & QI, L. 2010. Genome-wide association study identifies variants at the IL18-BCO2 locus associated with interleukin-18 levels. *Arterioscler Thromb Vasc Biol,* 30**,** 885-90.

IGLESIAS, A. I., VAN DER LEE, S. J., BONNEMAIJER, P. W. M., HOHN, R., NAG, A., GHARAHKHANI, P., KHAWAJA, A. P., BROER, L., INTERNATIONAL GLAUCOMA GENETICS, C., FOSTER, P. J., HAMMOND, C. J., HYSI, P. G., VAN LEEUWEN, E. M., MACGREGOR, S., MACKEY, D. A., MAZUR, J., NICKELS, S., UITTERLINDEN, A. G., KLAVER, C. C. W., AMIN, N. & VAN DUIJN, C. M. 2017. Haplotype reference consortium panel: Practical implications of imputations with large reference panels. *Hum Mutat,* 38**,** 1025-1032.

IKEDA, U. 2003. Inflammation and coronary artery disease. *Curr Vasc Pharmacol,* 1**,** 65-70.

JAMI, A. 2017. *Die Rolle der MicroRNA miR-1279 als multi-lokus Regulator in Monozyten.* Staats- und Universitätsbibliothek Hamburg.

JEFFERIS, B. J., PAPACOSTA, O., OWEN, C. G., WANNAMETHEE, S. G., HUMPHRIES, S. E., WOODWARD, M., LENNON, L. T., THOMSON, A., WELSH, P., RUMLEY, A., LOWE, G. D. & WHINCUP, P. H. 2011. Interleukin 18 and coronary heart disease: prospective study and systematic review. *Atherosclerosis,* 217**,** 227-33.

JOHANSSON, A., ERIKSSON, N., BECKER, R. C., STOREY, R. F., HIMMELMANN, A., HAGSTROM, E., VARENHORST, C., AXELSSON, T., BARRATT, B. J., JAMES, S. K., KATUS, H. A., STEG, P. G., SYVANEN, A. C., WALLENTIN, L., SIEGBAHN, A. & INVESTIGATORS, P. 2015. NLRC4 Inflammasome Is an Important Regulator of Interleukin-18 Levels in Patients With Acute Coronary Syndromes: Genome-Wide Association Study in the PLATelet inhibition and patient Outcomes Trial (PLATO). *Circ Cardiovasc Genet,* 8**,** 498-506.

KAUFMANN, R. 1995. Matrix-assisted laser desorption ionization (MALDI) mass spectrometry: a novel analytical tool in molecular biology and biotechnology. *J Biotechnol,* 41**,** 155-75.

KENT, W. J., SUGNET, C. W., FUREY, T. S., ROSKIN, K. M., PRINGLE, T. H., ZAHLER, A. M. & HAUSSLER, D. 2002. The human genome browser at UCSC. *Genome Res,* 12**,** 996-1006.

KERSSE, K., VANDEN BERGHE, T., LAMKANFI, M. & VANDENABEELE, P. 2007. A phylogenetic and functional overview of inflammatory caspases and caspase-1-related CARD-only proteins. *Biochem Soc Trans,* 35**,** 1508-11.

KESSLER, T., ERDMANN, J. & SCHUNKERT, H. 2013. Genetics of coronary artery disease and myocardial infarction--2013. *Curr Cardiol Rep,* 15**,** 368.

KOMINATO, Y., GALSON, D., WATERMAN, W. R., WEBB, A. C. & AURON, P. E. 1995. Monocyte expression of the human prointerleukin 1 beta gene (IL1B) is dependent on promoter sequences which bind the hematopoietic transcription factor Spi-1/PU.1. *Mol Cell Biol,* 15**,** 58-68.

KONG, Y., HSIEH, C. H. & ALONSO, L. C. 2018. ANRIL: A lncRNA at the CDKN2A/B Locus With Roles in Cancer and Metabolic Disease. *Front Endocrinol (Lausanne),* 9**,** 405.

KUMAR, Y., RADHA, V. & SWARUP, G. 2010. Interaction with Sug1 enables Ipaf ubiquitination leading to caspase 8 activation and cell death. *Biochem J,* 427**,** 91-104.

LAEMMLI, U. K. 1970. Cleavage of structural proteins during the assembly of the head of bacteriophage T4. *Nature,* 227**,** 680-5.

LASLETT, L. J., ALAGONA, P., JR., CLARK, B. A., 3RD, DROZDA, J. P., JR., SALDIVAR, F., WILSON, S. R., POE, C. & HART, M. 2012. The worldwide environment of

cardiovascular disease: prevalence, diagnosis, therapy, and policy issues: a report from the American College of Cardiology. *J Am Coll Cardiol,* 60**,** S1-49.

LATZ, E., XIAO, T. S. & STUTZ, A. 2013. Activation and regulation of the inflammasomes. *Nat Rev Immunol,* 13**,** 397-411.

LE, H. T. & HARTON, J. A. 2013. Pyrin- and CARD-only Proteins as Regulators of NLR Functions. *Front Immunol,* 4**,** 275.

LIBBY, P., RIDKER, P. M. & MASERI, A. 2002. Inflammation and atherosclerosis. *Circulation,* 105**,** 1135-43.

LIEBLER, D. C. & ZIMMERMAN, L. J. 2013. Targeted quantitation of proteins by mass spectrometry. *Biochemistry,* 52**,** 3797-806.

LINTON, M. F., YANCEY, P. G., DAVIES, S. S., JEROME, W. G. J., LINTON, E. F. & VICKERS, K. C. 2000. The Role of Lipids and Lipoproteins in Atherosclerosis. *In:* DE GROOT, L. J., CHROUSOS, G., DUNGAN, K., FEINGOLD, K. R., GROSSMAN, A., HERSHMAN, J. M., KOCH, C., KORBONITS, M., MCLACHLAN, R., NEW, M., PURNELL, J., REBAR, R., SINGER, F. & VINIK, A. (eds.) *Endotext.* South Dartmouth (MA).

LOH, P. R., DANECEK, P., PALAMARA, P. F., FUCHSBERGER, C., Y, A. R., H, K. F., SCHOENHERR, S., FORER, L., MCCARTHY, S., ABECASIS, G. R., DURBIN, R. & A, L. P. 2016. Reference-based phasing using the Haplotype Reference Consortium panel. *Nat Genet,* 48**,** 1443-1448.

LOZANO, R., NAGHAVI, M., FOREMAN, K., LIM, S., SHIBUYA, K., ABOYANS, V., ABRAHAM, J., ADAIR, T., AGGARWAL, R., AHN, S. Y., ALVARADO, M., ANDERSON, H. R., ANDERSON, L. M., ANDREWS, K. G., ATKINSON, C., BADDOUR, L. M., BARKER-COLLO, S., BARTELS, D. H., BELL, M. L., BENJAMIN, E. J., BENNETT, D., BHALLA, K., BIKBOV, B., BIN ABDULHAK, A., BIRBECK, G., BLYTH, F., BOLLIGER, I., BOUFOUS, S., BUCELLO, C., BURCH, M., BURNEY, P., CARAPETIS, J., CHEN, H., CHOU, D., CHUGH, S. S., COFFENG, L. E., COLAN, S. D., COLQUHOUN, S., COLSON, K. E., CONDON, J., CONNOR, M. D., COOPER, L. T., CORRIERE, M., CORTINOVIS, M., DE VACCARO, K. C., COUSER, W., COWIE, B. C., CRIQUI, M. H., CROSS, M., DABHADKAR, K. C., DAHODWALA, N., DE LEO, D., DEGENHARDT, L., DELOSSANTOS, A., DENENBERG, J., DES JARLAIS, D. C., DHARMARATNE, S. D., DORSEY, E. R., DRISCOLL, T., DUBER, H., EBEL, B., ERWIN, P. J., ESPINDOLA, P., EZZATI, M., FEIGIN, V., FLAXMAN, A. D., FOROUZANFAR, M. H., FOWKES, F. G., FRANKLIN, R., FRANSEN, M., FREEMAN, M. K., GABRIEL, S. E., GAKIDOU, E., GASPARI, F., GILLUM, R. F., GONZALEZ-MEDINA, D., HALASA, Y. A., HARING, D., HARRISON, J. E., HAVMOELLER, R., HAY, R. J., HOEN, B., HOTEZ, P. J., HOY, D., JACOBSEN, K. H., JAMES, S. L., JASRASARIA, R., JAYARAMAN, S., JOHNS, N., KARTHIKEYAN, G., KASSEBAUM, N., KEREN, A., KHOO, J. P., KNOWLTON, L. M., KOBUSINGYE, O., KORANTENG, A., KRISHNAMURTHI, R., LIPNICK, M., LIPSHULTZ, S. E., OHNO, S. L., et al. 2012. Global and regional mortality from 235 causes of death for 20 age groups in 1990 and 2010: a systematic analysis for the Global Burden of Disease Study 2010. *Lancet,* 380**,** 2095-128.

MALLAT, Z., CORBAZ, A., SCOAZEC, A., BESNARD, S., LESECHE, G., CHVATCHKO, Y. & TEDGUI, A. 2001. Expression of interleukin-18 in human atherosclerotic plaques and relation to plaque instability. *Circulation,* 104**,** 1598-603.

MALLAT, Z., HENRY, P., FRESSONNET, R., ALOUANI, S., SCOAZEC, A., BEAUFILS, P., CHVATCHKO, Y. & TEDGUI, A. 2002. Increased plasma concentrations of interleukin-18 in acute coronary syndromes. *Heart,* 88**,** 467-9.

MARCHINI, J., HOWIE, B., MYERS, S., MCVEAN, G. & DONNELLY, P. 2007. A new multipoint method for genome-wide association studies by imputation of genotypes. *Nat Genet,* 39**,** 906-13.

MARTINON, F., BURNS, K. & TSCHOPP, J. 2002. The inflammasome: a molecular platform triggering activation of inflammatory caspases and processing of proIL-beta. *Mol Cell,* 10**,** 417-26.

MATTEINI, A. M., LI, J., LANGE, E. M., TANAKA, T., LANGE, L. A., TRACY, R. P., WANG, Y., BIGGS, M. L., ARKING, D. E., FALLIN, M. D., CHAKRAVARTI, A., PSATY, B. M., BANDINELLI, S., FERRUCCI, L., REINER, A. P. & WALSTON, J. D. 2014. Novel gene variants predict serum levels of the cytokines IL-18 and IL-1ra in older adults. *Cytokine,* 65**,** 10-6.

MIAO, E. A. & RAJAN, J. V. 2011. Salmonella and Caspase-1: A complex Interplay of Detection and Evasion. *Front Microbiol,* 2**,** 85.

MONIE, T. P. 2017. The Canonical Inflammasome: A Macromolecular Complex Driving Inflammation. *Subcell Biochem,* 83**,** 43-73.

MOORE, K. J., SHEEDY, F. J. & FISHER, E. A. 2013. Macrophages in atherosclerosis: a dynamic balance. *Nat Rev Immunol,* 13**,** 709-21.

NAKANISHI, K., YOSHIMOTO, T., TSUTSUI, H. & OKAMURA, H. 2001. Interleukin-18 regulates both Th1 and Th2 responses. *Annu Rev Immunol,* 19**,** 423-74.

NIKPAY, M., GOEL, A., WON, H. H., HALL, L. M., WILLENBORG, C., KANONI, S., SALEHEEN, D., KYRIAKOU, T., NELSON, C. P., HOPEWELL, J. C., WEBB, T. R., ZENG, L., DEHGHAN, A., ALVER, M., ARMASU, S. M., AURO, K., BJONNES, A., CHASMAN, D. I., CHEN, S., FORD, I., FRANCESCHINI, N., GIEGER, C., GRACE, C., GUSTAFSSON, S., HUANG, J., HWANG, S. J., KIM, Y. K., KLEBER, M. E., LAU, K. W., LU, X., LU, Y., LYYTIKAINEN, L. P., MIHAILOV, E., MORRISON, A. C., PERVJAKOVA, N., QU, L., ROSE, L. M., SALFATI, E., SAXENA, R., SCHOLZ, M., SMITH, A. V., TIKKANEN, E., UITTERLINDEN, A., YANG, X., ZHANG, W., ZHAO, W., DE ANDRADE, M., DE VRIES, P. S., VAN ZUYDAM, N. R., ANAND, S. S., BERTRAM, L., BEUTNER, F., DEDOUSSIS, G., FROSSARD, P., GAUGUIER, D., GOODALL, A. H., GOTTESMAN, O., HABER, M., HAN, B. G., HUANG, J., JALILZADEH, S., KESSLER, T., KONIG, I. R., LANNFELT, L., LIEB, W., LIND, L., LINDGREN, C. M., LOKKI, M. L., MAGNUSSON, P. K., MALLICK, N. H., MEHRA, N., MEITINGER, T., MEMON, F. U., MORRIS, A. P., NIEMINEN, M. S., PEDERSEN, N. L., PETERS, A., RALLIDIS, L. S., RASHEED, A., SAMUEL, M., SHAH, S. H., SINISALO, J., STIRRUPS, K. E., TROMPET, S., WANG, L., ZAMAN, K. S., ARDISSINO, D., BOERWINKLE, E., BORECKI, I. B., BOTTINGER, E. P., BURING, J. E., CHAMBERS, J. C., COLLINS, R., CUPPLES, L. A., DANESH, J., DEMUTH, I., ELOSUA, R., EPSTEIN, S. E., ESKO, T., FEITOSA, M. F., et al. 2015. A comprehensive 1,000 Genomes-based genome-wide association meta-analysis of coronary artery disease. *Nat Genet,* 47**,** 1121-1130.

OKAMURA, H., TSUTSI, H., KOMATSU, T., YUTSUDO, M., HAKURA, A., TANIMOTO, T., TORIGOE, K., OKURA, T., NUKADA, Y., HATTORI, K. & ET AL. 1995. Cloning of a new cytokine that induces IFN-gamma production by T cells. *Nature,* 378**,** 88-91.

PROMEGA 2015. Technical Manual Dual-Luciferse ® Reporter Assay Systems: Bioluminescent reactions catalyzed by firefly luciferases. 2015: Promega.

QU, Y., MISAGHI, S., IZRAEL-TOMASEVIC, A., NEWTON, K., GILMOUR, L. L., LAMKANFI, M., LOUIE, S., KAYAGAKI, N., LIU, J., KOMUVES, L., CUPP, J. E., ARNOTT, D., MONACK, D. & DIXIT, V. M. 2012. Phosphorylation of NLRC4 is critical for inflammasome activation. *Nature,* 490**,** 539-42.

RAMANI, T., AULETTA, C. S., WEINSTOCK, D., MOUNHO-ZAMORA, B., RYAN, P. C., SALCEDO, T. W. & BANNISH, G. 2015. Cytokines: The Good, the Bad, and the Deadly. *Int J Toxicol,* 34**,** 355-65.

RAPSOMANIKI, E., TIMMIS, A., GEORGE, J., PUJADES-RODRIGUEZ, M., SHAH, A. D., DENAXAS, S., WHITE, I. R., CAULFIELD, M. J., DEANFIELD, J. E., SMEETH, L., WILLIAMS, B., HINGORANI, A. & HEMINGWAY, H. 2014. Blood pressure and incidence of twelve cardiovascular diseases: lifetime risks, healthy life-years lost, and age-specific associations in 1.25 million people. *Lancet,* 383**,** 1899-911.

RIDKER, P. M. 2017. How Common Is Residual Inflammatory Risk? *Circ Res,* 120**,** 617-619.

RIDKER, P. M., EVERETT, B. M., THUREN, T., MACFADYEN, J. G., CHANG, W. H., BALLANTYNE, C., FONSECA, F., NICOLAU, J., KOENIG, W., ANKER, S. D., KASTELEIN, J. J. P., CORNEL, J. H., PAIS, P., PELLA, D., GENEST, J., CIFKOVA, R., LORENZATTI, A., FORSTER, T., KOBALAVA, Z., VIDA-SIMITI, L., FLATHER, M., SHIMOKAWA, H., OGAWA, H., DELLBORG, M., ROSSI, P. R. F., TROQUAY, R. P. T., LIBBY, P., GLYNN, R. J. & GROUP, C. T. 2017. Antiinflammatory Therapy with Canakinumab for Atherosclerotic Disease. *N Engl J Med,* 377**,** 1119-1131.

ROSS, R. 1995. Cell biology of atherosclerosis. *Annu Rev Physiol,* 57**,** 791-804.

SALOMAA, V., HAVULINNA, A., SAARELA, O., ZELLER, T., JOUSILAHTI, P., JULA, A., MUENZEL, T., AROMAA, A., EVANS, A., KUULASMAA, K. & BLANKENBERG, S. 2010. Thirty-one novel biomarkers as predictors for clinically incident diabetes. *PLoS One,* 5**,** e10100.

SAMANI, N. J., ERDMANN, J., HALL, A. S., HENGSTENBERG, C., MANGINO, M., MAYER, B., DIXON, R. J., MEITINGER, T., BRAUND, P., WICHMANN, H. E., BARRETT, J. H., KONIG, I. R., STEVENS, S. E., SZYMCZAK, S., TREGOUET, D. A., ILES, M. M., PAHLKE, F., POLLARD, H., LIEB, W., CAMBIEN, F., FISCHER, M., OUWEHAND, W., BLANKENBERG, S., BALMFORTH, A. J., BAESSLER, A., BALL, S. G., STROM, T. M., BRAENNE, I., GIEGER, C., DELOUKAS, P., TOBIN, M. D., ZIEGLER, A., THOMPSON, J. R., SCHUNKERT, H., WTCCC & THE CARDIOGENICS, C. 2007. Genomewide association analysis of coronary artery disease. *N Engl J Med,* 357**,** 443-53.

SHAPIRO, M. D. & FAZIO, S. 2016. From Lipids to Inflammation: New Approaches to Reducing Atherosclerotic Risk. *Circ Res,* 118**,** 732-49.

SHASHKIN, P., DRAGULEV, B. & LEY, K. 2005. Macrophage differentiation to foam cells. *Curr Pharm Des,* 11**,** 3061-72.

SONG, G., WANG, L., BI, K. & JIANG, G. 2015. Regulation of the C/EBPalpha signaling pathway in acute myeloid leukemia (Review). *Oncol Rep,* 33**,** 2099-106.

STARY, H. C. 1994. Changes in components and structure of atherosclerotic lesions developing from childhood to middle age in coronary arteries. *Basic Res Cardiol,* 89 Suppl 1**,** 17-32.

STEINL, D. C. & KAUFMANN, B. A. 2015. Ultrasound imaging for risk assessment in atherosclerosis. *Int J Mol Sci,* 16**,** 9749-69.

STROWIG, T., HENAO-MEJIA, J., ELINAV, E. & FLAVELL, R. 2012. Inflammasomes in health and disease. *Nature,* 481**,** 278-86.

SZKLARCZYK, D., MORRIS, J. H., COOK, H., KUHN, M., WYDER, S., SIMONOVIC, M., SANTOS, A., DONCHEVA, N. T., ROTH, A., BORK, P., JENSEN, L. J. & VON MERING, C. 2017. The STRING database in 2017: quality-controlled protein-protein association networks, made broadly accessible. *Nucleic Acids Res,* 45**,** D362-D368.

TIRET, L., GODEFROY, T., LUBOS, E., NICAUD, V., TREGOUET, D. A., BARBAUX, S., SCHNABEL, R., BICKEL, C., ESPINOLA-KLEIN, C., POIRIER, O., PERRET, C., MUNZEL, T., RUPPRECHT, H. J., LACKNER, K., CAMBIEN, F.,

BLANKENBERG, S. & ATHEROGENE, I. 2005. Genetic analysis of the interleukin-18 system highlights the role of the interleukin-18 gene in cardiovascular disease. *Circulation,* 112**,** 643-50.

WANG, C., CHEN, H., LUO, H., ZHU, L., ZHAO, Y., TIAN, H., WANG, R., SHANG, P. & ZHAO, Y. 2015. Microgravity activates p38 MAPK-C/EBPbeta pathway to regulate the expression of arginase and inflammatory cytokines in macrophages. *Inflamm Res,* 64**,** 303-11.

WEIDMANN, H., TOUAT-HAMICI, Z., DURAND, H., MUELLER, C., CHARDONNET, S., PIONNEAU, C., CHARLOTTE, F., JANSSEN, K. P., VERDUGO, R., CAMBIEN, F., BLANKENBERG, S., TIRET, L., ZELLER, T. & NINIO, E. 2015. SASH1, a new potential link between smoking and atherosclerosis. *Atherosclerosis,* 242**,** 571-9.

WINKLER, S. & ROSEN-WOLFF, A. 2015. Caspase-1: an integral regulator of innate immunity. *Semin Immunopathol,* 37**,** 419-27.

WITTE, J. S. 2010. Genome-wide association studies and beyond. *Annu Rev Public Health,* 31**,** 9-20 4 p following 20.

YAHAGI, K., DAVIS, H. R., ARBUSTINI, E. & VIRMANI, R. 2015. Sex differences in coronary artery disease: pathological observations. *Atherosclerosis,* 239**,** 260-7.

ZELLER, T., HAASE, T., MULLER, C., RIESS, H., LAU, D., ZELLER, S., KRAUSE, J., BAUMERT, J., PLESS, O., DUPUIS, J., WILD, P. S., ELEFTHERIADIS, M., WALDENBERGER, M., ZEILINGER, S., ZIEGLER, A., PETERS, A., TIRET, L., PROUST, C., MARZI, C., MUNZEL, T., STRAUCH, K., PROKISCH, H., LACKNER, K. J., HERDER, C., THORAND, B., BENJAMIN, E. J., BLANKENBERG, S., KOENIG, W. & SCHNABEL, R. B. 2015. Molecular Characterization of the NLRC4 Expression in Relation to Interleukin-18 Levels. *Circ Cardiovasc Genet,* 8**,** 717-26.

ZHAO, Y., YANG, J., SHI, J., GONG, Y. N., LU, Q., XU, H., LIU, L. & SHAO, F. 2011. The NLRC4 inflammasome receptors for bacterial flagellin and type III secretion apparatus. *Nature,* 477**,** 596-600.

ZHU, G., CHEN, J., TIAN, J., GE, L., XING, A. & TANG, G. 2016. Expression of NLRC4 in children with septicaemia and mechanisms of NLRC4 in in vitro cytokine secretion. *Mol Med Rep,* 14**,** 509-14.

Teilergebnisse der vorliegenden Arbeit wurden in folgender Originalarbeit

ZELLER, T., HAASE, T., MULLER, C., RIESS, H., LAU, D., **ZELLER, S.**, KRAUSE, J., BAUMERT, J., PLESS, O., DUPUIS, J., WILD, P. S., ELEFTHERIADIS, M., WALDENBERGER, M., ZEILINGER, S., ZIEGLER, A., PETERS, A., TIRET, L., PROUST, C., MARZI, C., MUNZEL, T., STRAUCH, K., PROKISCH, H., LACKNER, K. J., HERDER, C., THORAND, B., BENJAMIN, E. J., BLANKENBERG, S., KOENIG, W. & SCHNABEL, R. B. 2015. Molecular Characterization of the NLRC4 Expression in Relation to Interleukin-18 Levels. *Circ Cardiovasc Genet,* 8**,** 717-26.

Circulation: Genomic and Precicion Medicine (ehemals Circulation: Cardiovascular Genetics) ist ein Journal der American Heart Association (AHA). Für die Nutzung von (Teil-) Ergebnissen einer publizierten Arbeit nach Veröffentlichung im Journal besteht folgende Aussage (Stand Dezember, 2018): http://circgenetics.ahajournals.org/content/permissions-rights-q-and-a

und folgenden Kongressbeitrag veröffentlicht:

ZELLER, S. M., C.; LAU, D.; SCHABEL, R.; WILD, P. S.; LACKNER, K. J.; MÜNZEL, T.; BLANKENBERG, S.; ZELLER, T. 2013. The role of the NLRC4 Inflammasome on the pathogenesis of coronary disease: the influence of genetic variations. *79. Jahrestagung der Deutschen Gesellschaft für Kardiologie.* Mannheim, Germany.

9 Danksagung

Im Besonderen möchte Frau Prof. Dr. Tanja Zeller für die Möglichkeit, diese Arbeit anfertigen zu können danken. Ihre Betreuung mit klarer Leitung, Rat und unendlicher Geduld haben die Ausarbeitung erst ermöglicht.

Frau Dr. Denise Lau möchte ich im Besonderen dafür danken, dass sie mit ihrer unendlichen Erfahrung zu jeder Zeit für nahezu jedes Problem eine Lösung fand. Herrn Christian Müller möchte ich dafür danken, dass er die Auswertung dieser Arbeit essenziell ermöglichte. Danken möchte ich ihm jedoch auch für die unzählbar vielen fachlichen und nicht-fachlichen Gespräche, und seine Unterstützung bis zum Schluss. Herrn Dr. Henri Weidmann möchte ich im Besonderen dafür danken, dass nicht nur seine Erfahrung, sondern auch seine Persönlichkeit und Kreativität diese Arbeit kontinuierlich, zu jeder Zeit und an jedem Ort nach vorne gebracht hat.

Dem gesamten Team der AG Molekulare Kardiologie - Genomik und Systemmedizin möchte ich für die stete Unterstützung und die angenehme Gesellschaft im und außerhalb des Labors danken.

-

Zuletzt möchte ich meiner Familie aufrichtig und von ganzem Herzen für ihre liebevolle und unbeirrbare Unterstützung danken und widme ihr diese Dissertation.

-

10 Eidesstattliche Versicherung

Ich versichere ausdrücklich, dass ich die Arbeit selbständig und ohne fremde Hilfe verfasst, andere als die von mir angegebenen Quellen und Hilfsmittel nicht benutzt und die aus den benutzten Werken wörtlich oder inhaltlich entnommenen Stellen einzeln nach Ausgabe (Auflage und Jahr des Erscheinens), Band und Seite des benutzten Werkes kenntlich gemacht habe.
Ferner versichere ich, dass ich die Dissertation bisher nicht einem Fachvertreter an einer anderen Hochschule zur Überprüfung vorgelegt oder mich anderweitig um Zulassung zur Promotion beworben habe.
Ich erkläre mich einverstanden, dass meine Dissertation vom Dekanat der Medizinischen Fakultät mit einer gängigen Software zur Erkennung von Plagiaten überprüft werden kann.

Unterschrift: .....